



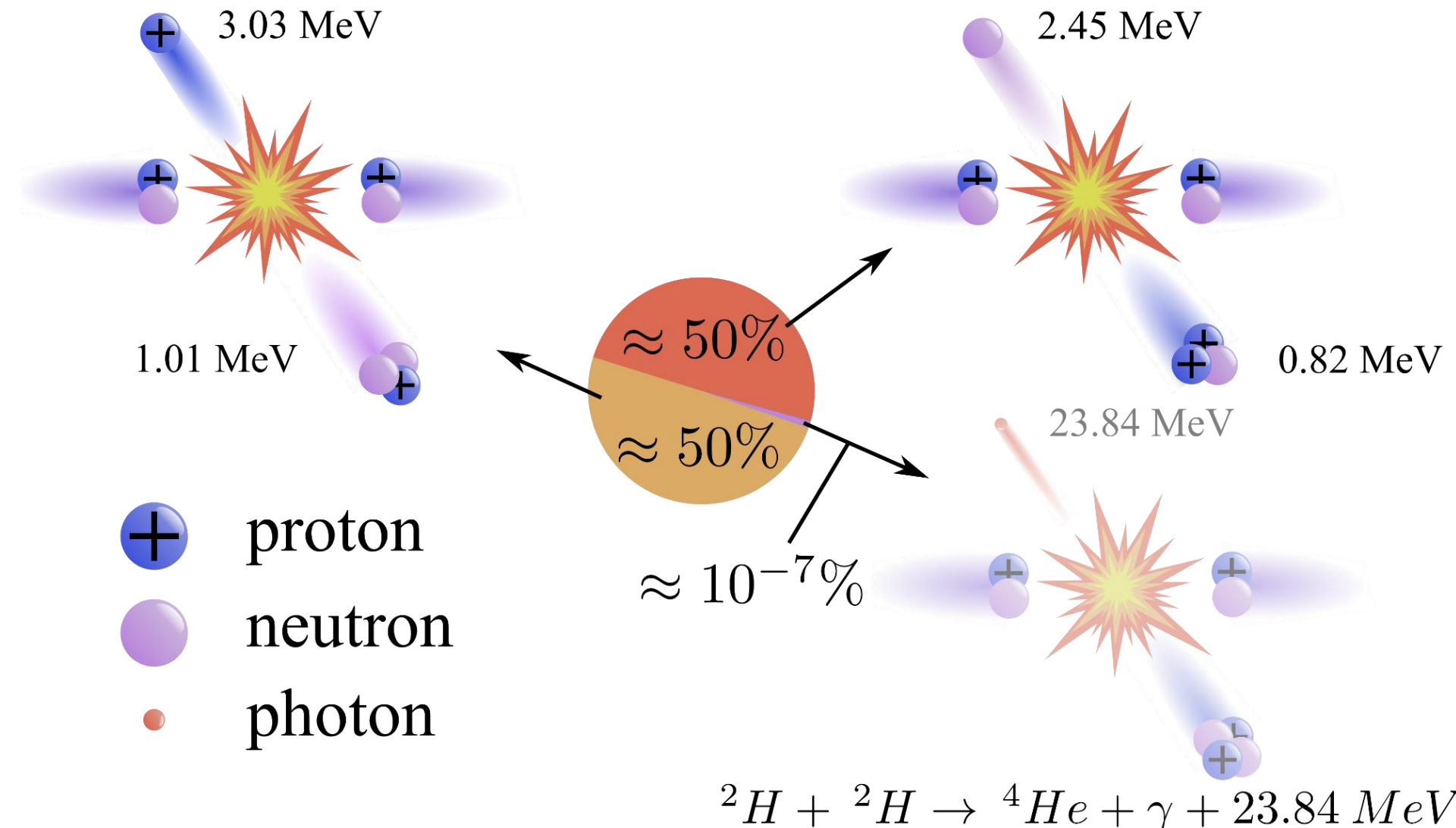
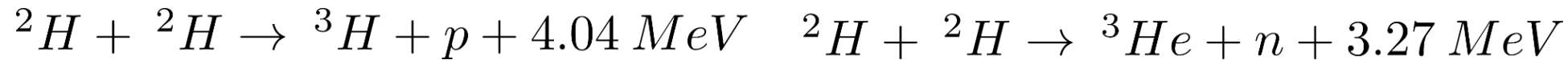
Development of a system of scintillation detectors for space radiation suppression in the experiment aims to study dd-fusion reactions with the low beam energy (PolFusion)

A. Rozhdestvenskij,
A. Vasilyev, M. Vznuzdaev, K. Ivshin, L. Kochenda, P. Kravtsov,
P. Kravchenko, V. Larionov, A. Solovev, V. Trofimov, V. Fotev

Petersburg Nuclear Physics Institute
Gatchina, Russia



DD-fusion reactions





Applied and fundamental physics

Astrophysics

- Big Bang
- Hydrogen burning
- Helium burning
- Advanced burning
- (carbon/neon/oxygen/silicon)
- s-process (neutron sources)
- p-process

Theory of nuclear interaction

- Wide range of models
- Difficulties in describing direct/indirect measurements

Thermonuclear energy

- Use of polarized fuel
- Cross section increase
- Controlling the Angular Distribution of Escape of Reaction Products
- Reactors with low neutron yield

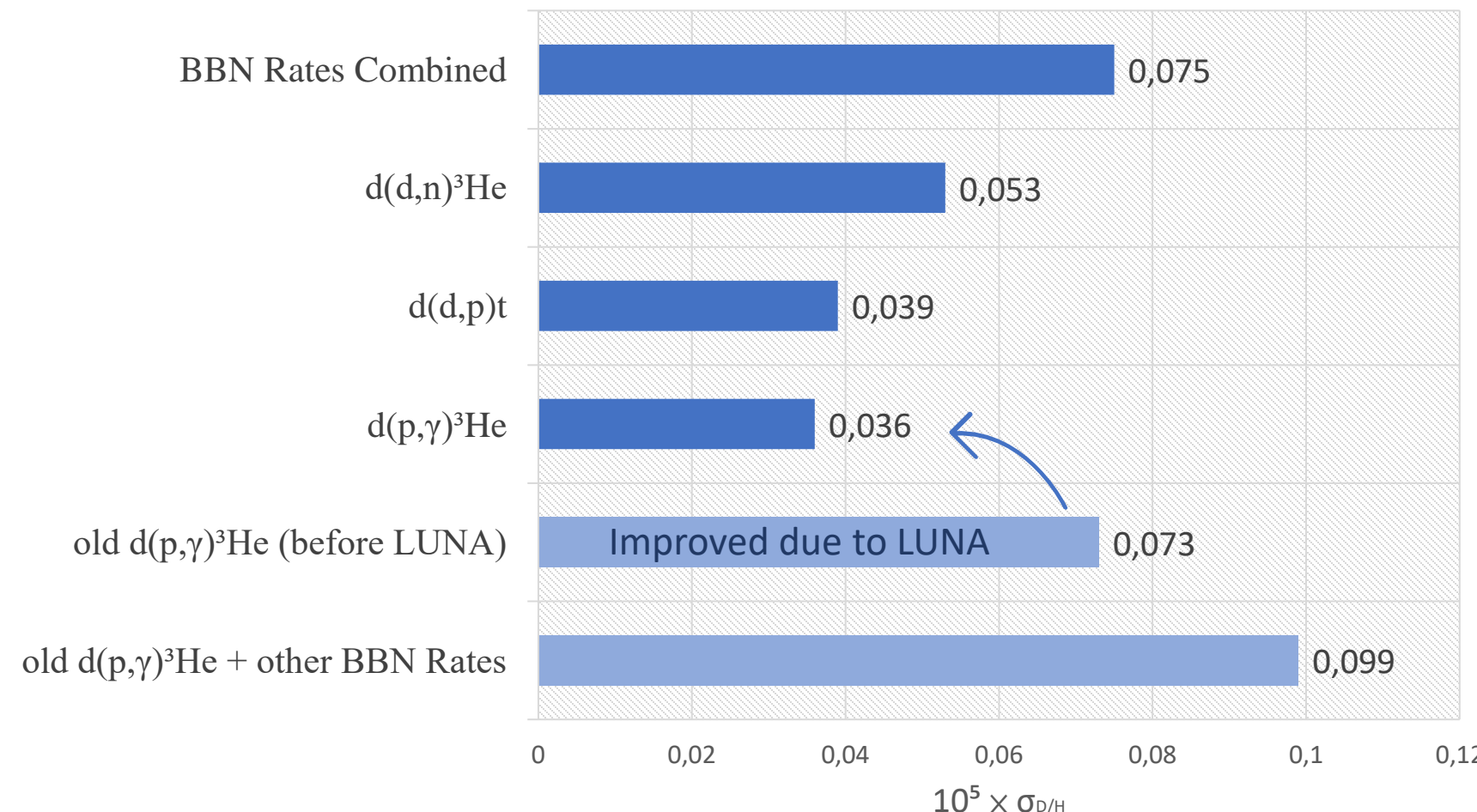
Applied physics

- Tritium and helium-3 production
- ^3He -oriented technology of gas-discharge detectors
- Neutron source to produce medical isotopes $^{100}\text{Mo}(\text{n},2\text{n})^{99}\text{Mo}$



Big Bang nucleosynthesis \longrightarrow Primordial isotope ratio D/H

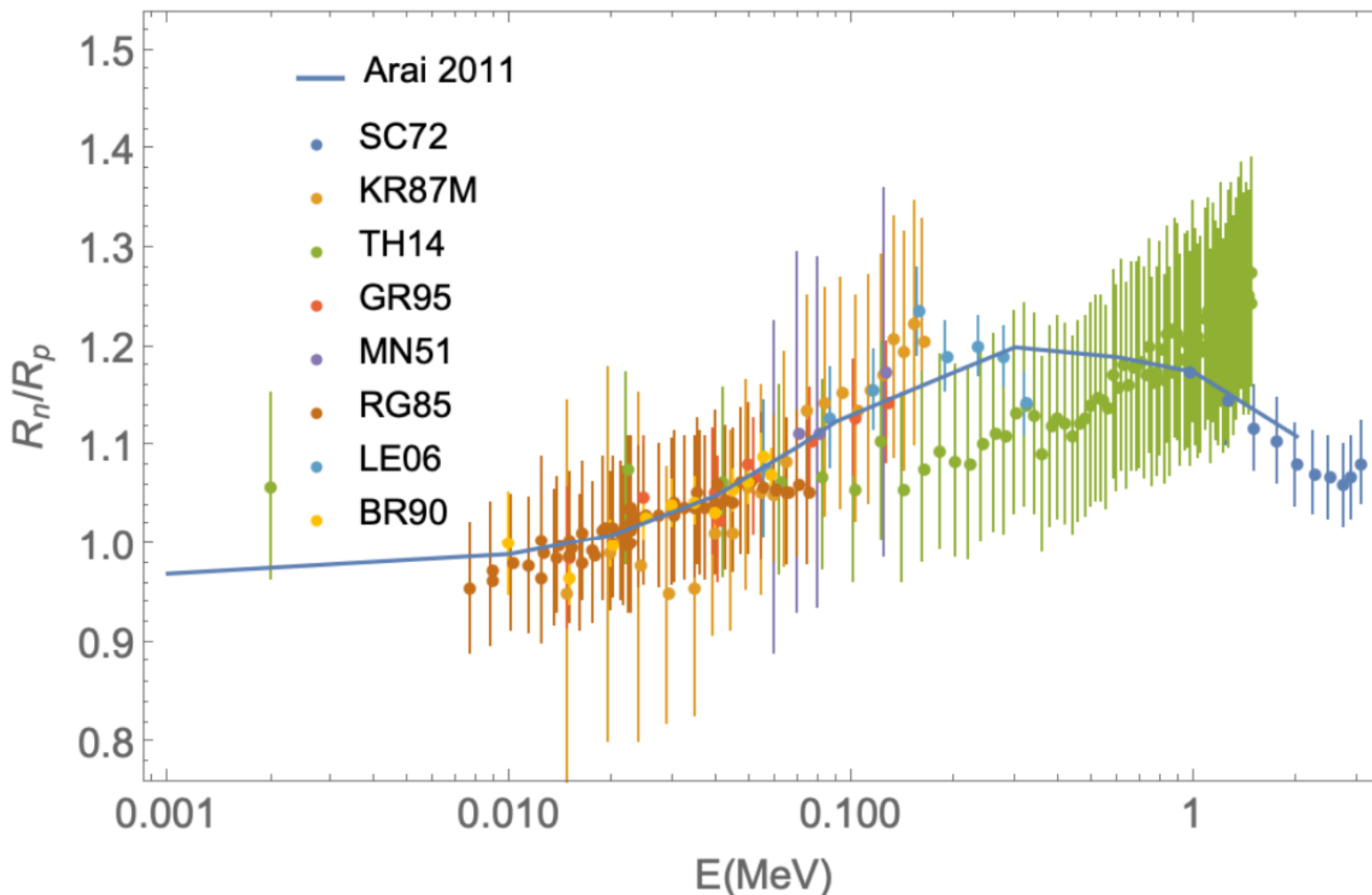
Deuterium Uncertainty Contributions



Better dd-data
needed!



Astrophysics



Ratios of processes $d(d, n)^3\text{He}$ to $d(d, p)^3\text{H}$
S-factors from experiments (dots) and
theory (solid line). The Trojan Horse points
from with their $1-\sigma$ errors are shown in
green (TH).



**New dd (both channels)
measurements needed!**

Theory prediction: K. Arai, S. Aoyama,
Y. Suzuki, P. Descouvemont, and D.
Baye Phys. Rev. Lett. 107, 132502
(2011)

Ofelia Pisanti, Gianpiero Mangano, Gennaro Miele, and Pierpaolo Mazzella
Primordial Deuterium after LUNA: concordances and error budget (2020)



Theoretical methods

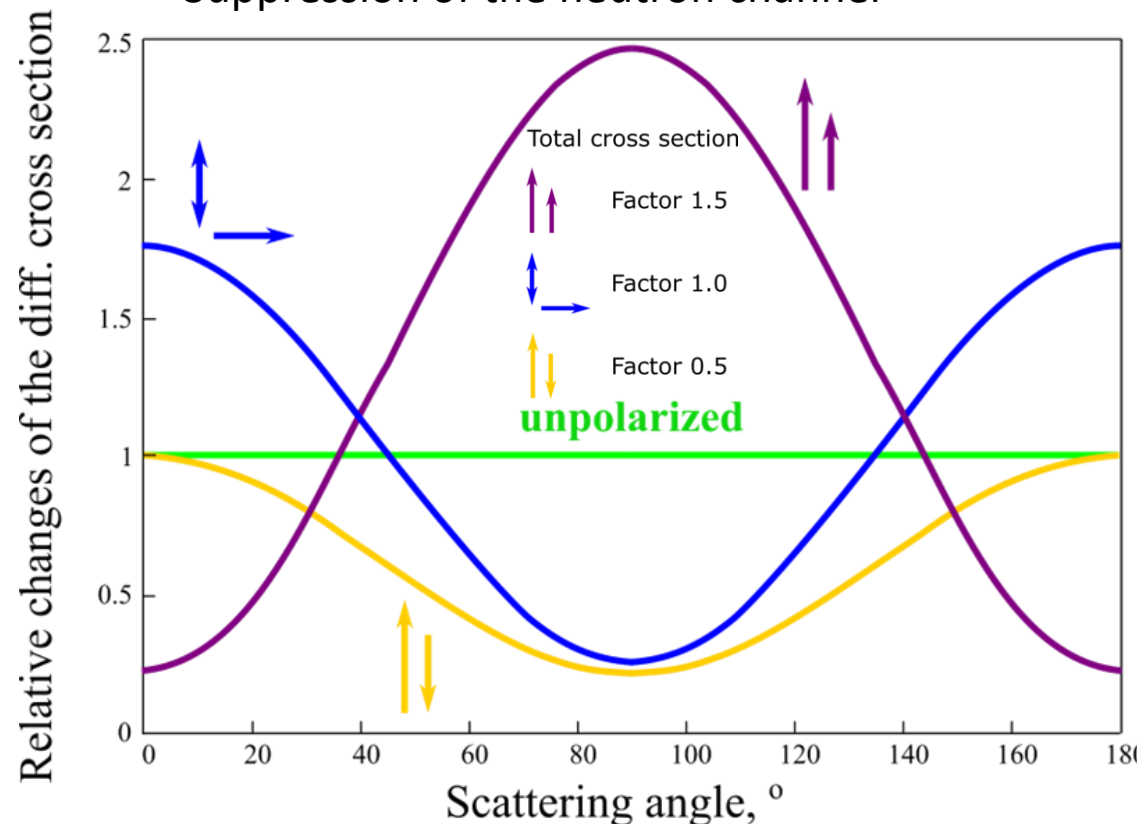
Many different cases → No “unique” model

Model	Applicable to	Comments
Potential/optical model	Capture Fusion	<ul style="list-style-type: none">• Internal structure neglected• Antisymmetrization approximated
R-matrix	Capture Transfer	<ul style="list-style-type: none">• No explicit wave function• Physics simulated by some parameters
DWBA	Transfer	<ul style="list-style-type: none">• Perturbation method• Wave function in the entrance and exit channels
Microscopic models	Capture Transfer	<ul style="list-style-type: none">• Based on a nucleon-nucleon interaction• A-nucleon problems• Predictive power

Pierre Descouvemont: Reaction models in nuclear astrophysics

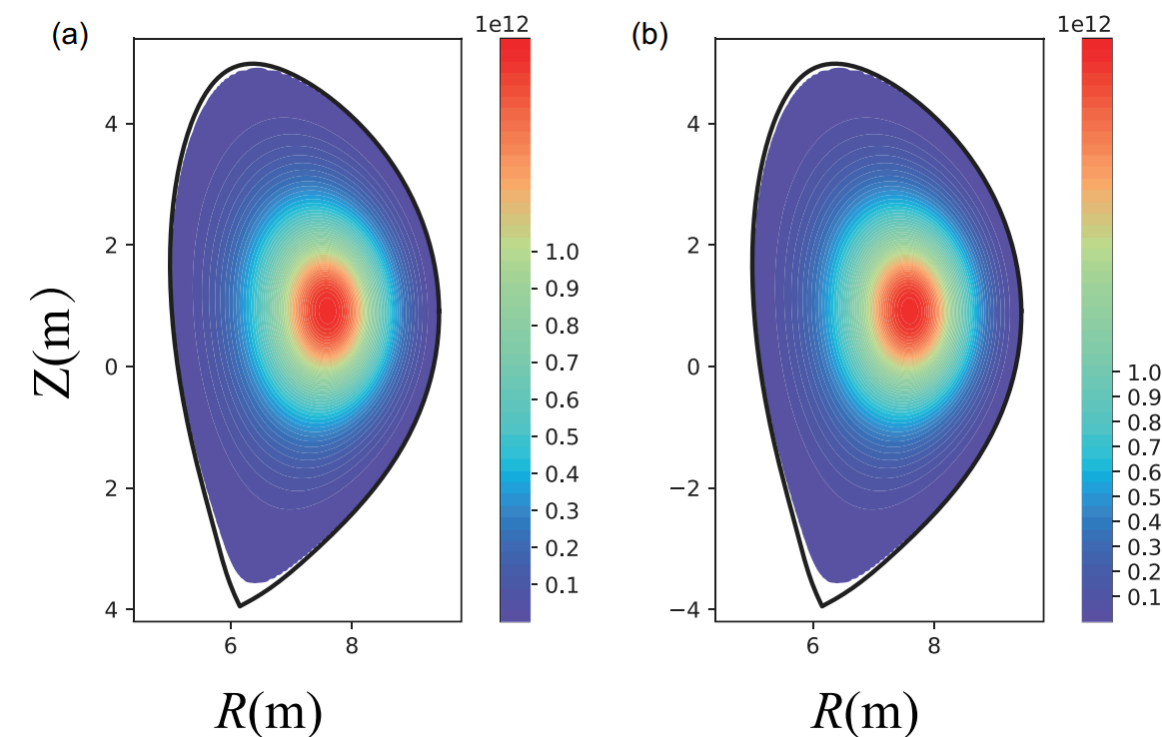
Thermonuclear fusion and applied physics

- Cross section increasement
- Control over the direction of expansion of reaction products
- Suppression of the neutron channel



Exp.: Ch. Leemann et al., Helv. Phys. Acta **44**, 141 (1971)
Theor.: G. Hupin et al. Nature Com. **10**, 321 (2019)

Distributions of neutron sources in coordinates (R , Z) for
(a) non-polarized case and (b) case of full parallel polarization



W.Yang, G.Li, X.Gong, X.Gao, X.Li, H.Li... Effect of the Fusion Fuels' Polarization on Neutron Wall Loading Distribution in CFETR (2021)
<https://doi.org/10.1080/15361055.2021.1969064> (China Fusion Engineering Test Reactor (CFETR))



Review of experiments

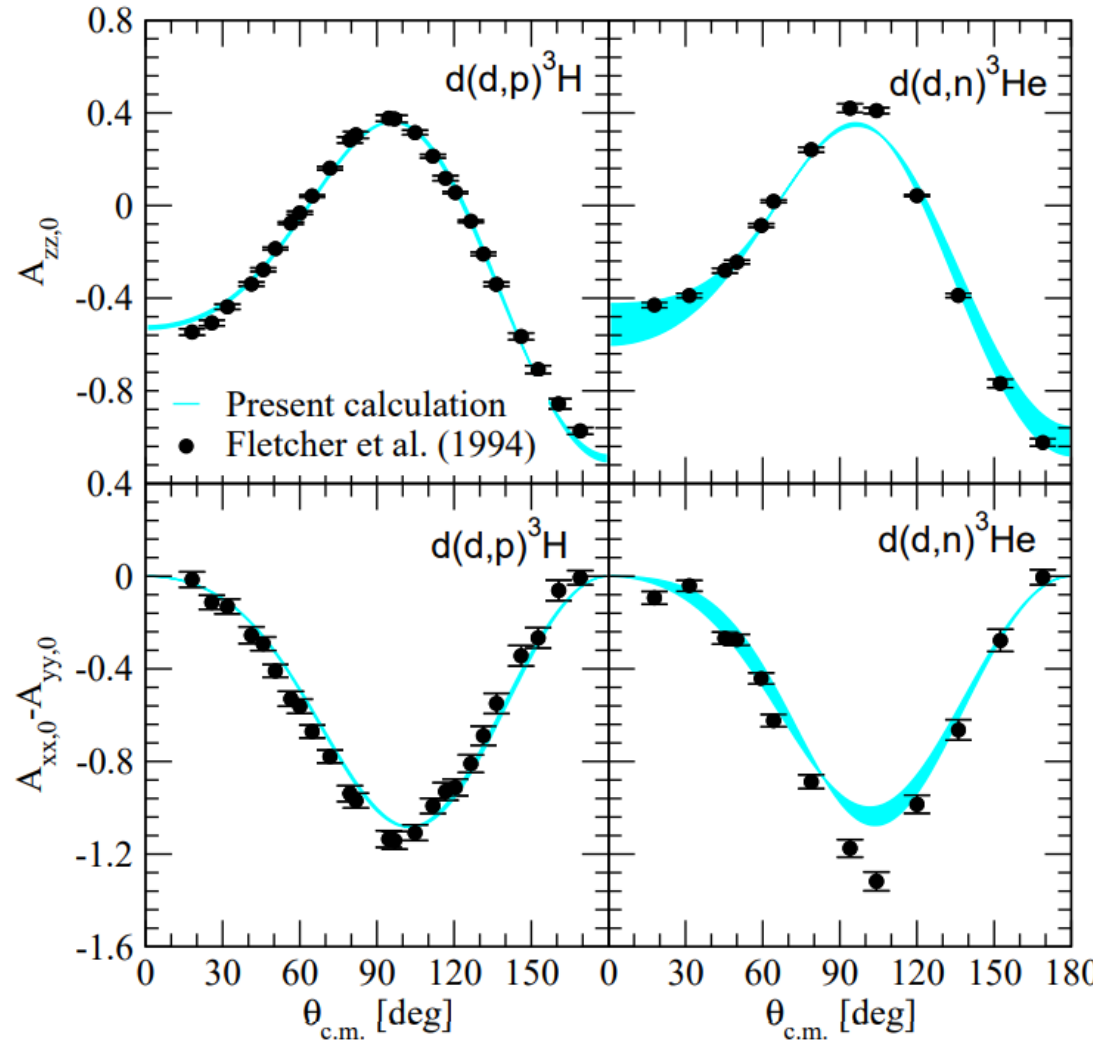
$$\sigma(\theta, \phi) = \sigma_0(\theta) \left(1 + \sum_1^9 p_j^b A_j^b(\theta) + \sum_1^9 p_j^t A_j^t(\theta) + \sum_1^9 \sum_1^9 p_j^b p_k^t C_{j,k}(\theta) \right)$$

$$p_{l'} \sigma(\theta, \phi) = \sigma_0(\theta) \left(P_{l'}(\theta) + \sum_1^9 p_j K_j^{l'}(\theta) \right)$$

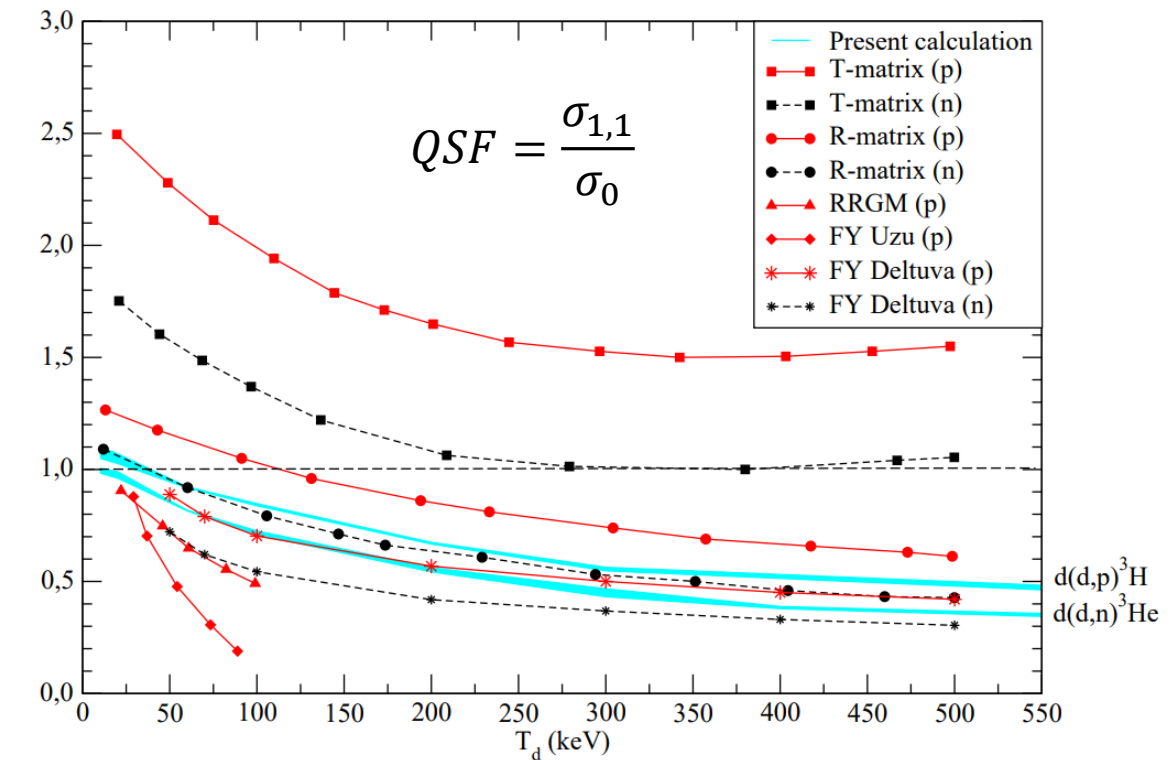
Experiment	Observable		
${}^2\vec{H}(\vec{d}, p){}^3H$ ${}^2\vec{H}(\vec{d}, n){}^3He$	$C_{z,z}$ $C_{y,y}$ $C_{zz,zz}$ $C_{y,zz}$ $C_{y,xz}$ $C_{zz,xz}$		p-channel n-channel
${}^2H(\vec{d}, \vec{p}){}^3H$ ${}^2H(\vec{d}, \vec{n}){}^3He$	$K_y^{x'}$ $K_y^{y'}$ $K_{xz}^{z'}$...		Imig A. et al., Phys. Rev. C 73, 024001 (2006) Katabuchi T. et al., Phys. Rev. C 64, 047601 (2001)
${}^2H(\vec{d}, p){}^3H$ ${}^2H(\vec{d}, n){}^3He$	A_y A_{xz} A_{zz} $A_{xx} - A_{yy}$		Tagishi Y. et al., Nucl. Instrum. Methods Phys. Res. A 402, 436 (1998) Fletcher K. A. et al., Phys. Rev. C 49, 2305 (1994) Tagishi Y. et al., Phys. Rev. C 46, R1155 (1992) Becker B. et al., Few-Body Syst. 13, 19 (1992)
${}^2H(d, \vec{p}){}^3H$ ${}^2H(d, \vec{n}){}^3He$	$P^{x'}$ $P^{y'}$ $P^{z'}$		Behof A. F., May T. H., McGarry W. I., Nucl. Phys. A108, 250 (1968) Haegusgen H., et al., Nucl. Phys. 73, 417 (1965) Rogers J. T. and Bond C. D., Nuclear Physics 53 (1964) 297 Kane P. P., Nuclear Physics 10 (1959) 429
${}^2H(d, p){}^3H$ ${}^2H(d, n){}^3He$	σ_0 $\frac{d\sigma}{d\Omega}$		Brown R. E. and N. Jarmie, Phys. Rev. C 41, 1391 (1990) Krauss A. et al., Nucl. Phys. A465, 150 (1987) Theus R. B., W. I. McGarry, and L. A. Beach, Nucl. Phys. 80, 273 (1966) McNeill K. G., Phil. Mag. 46 (1955) 800; Arnold W. R. et al., Phys. Rev. 93 (1954) 483 Moffat J., D. Roaf and J. H. Sanders, Proc. Roy. Soc. A212 (1952) 220 Wenzel W. A. and W. Whaling, Phys. Rev. 88 (1952) 1149 Bretscher E., A. P. French and F. G. P. Seidl, Phys. Rev. 73 (1948) 815



Latest research



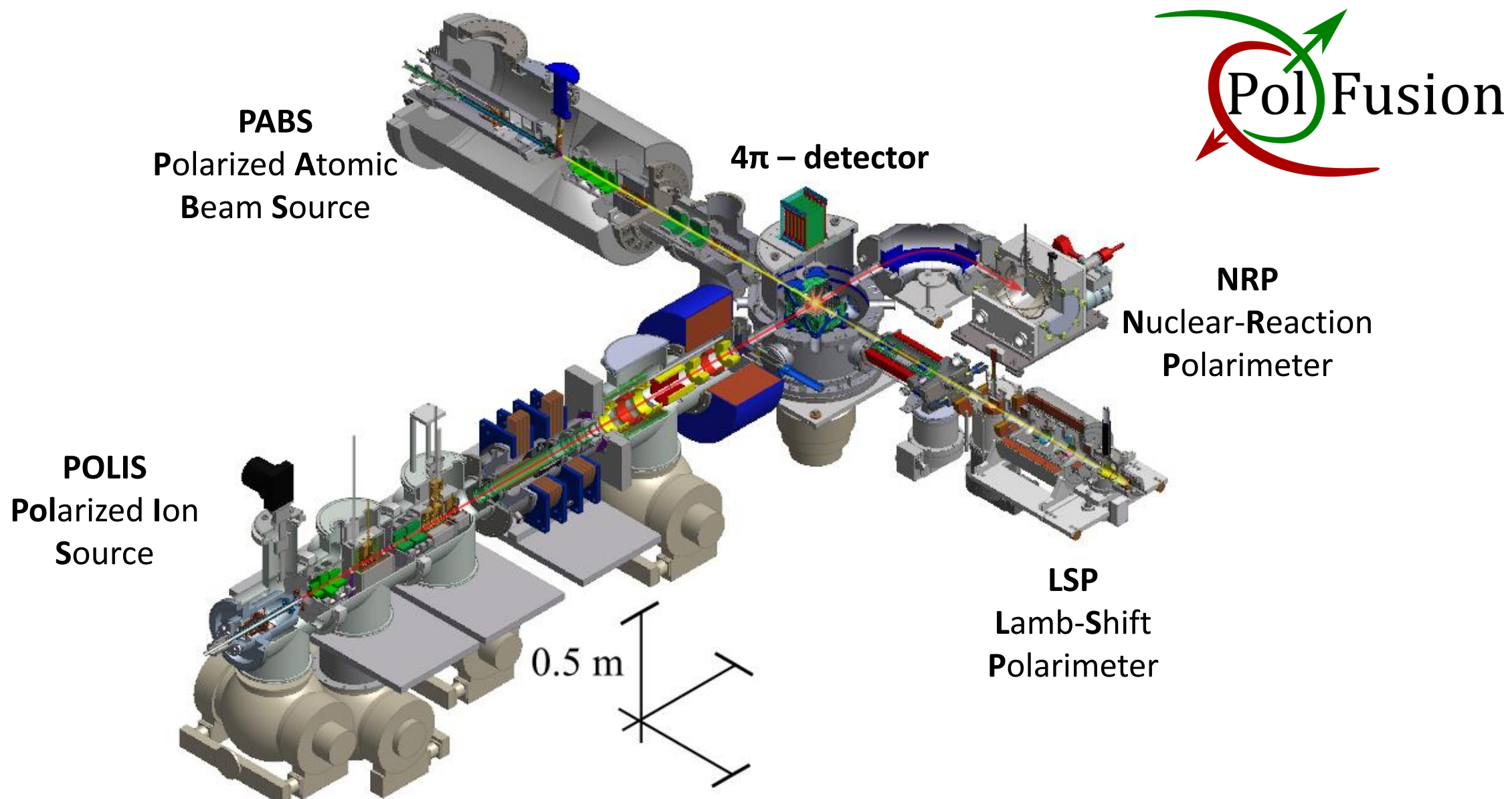
The observables $A_{zz,0}$ and $A_{xx,0} - A_{yy,0}$ for the \vec{d} (d , p) ${}^3\text{H}$ and \vec{d} (d , n) ${}^3\text{He}$ processes at $T_d = 21$ keV. The (cyan) bands show the results of the present calculations.



The QSF for the processes $d(d, n)$ ${}^3\text{He}$ and $d(d, p)$ ${}^3\text{H}$.



Experimental setup





Experimental setup

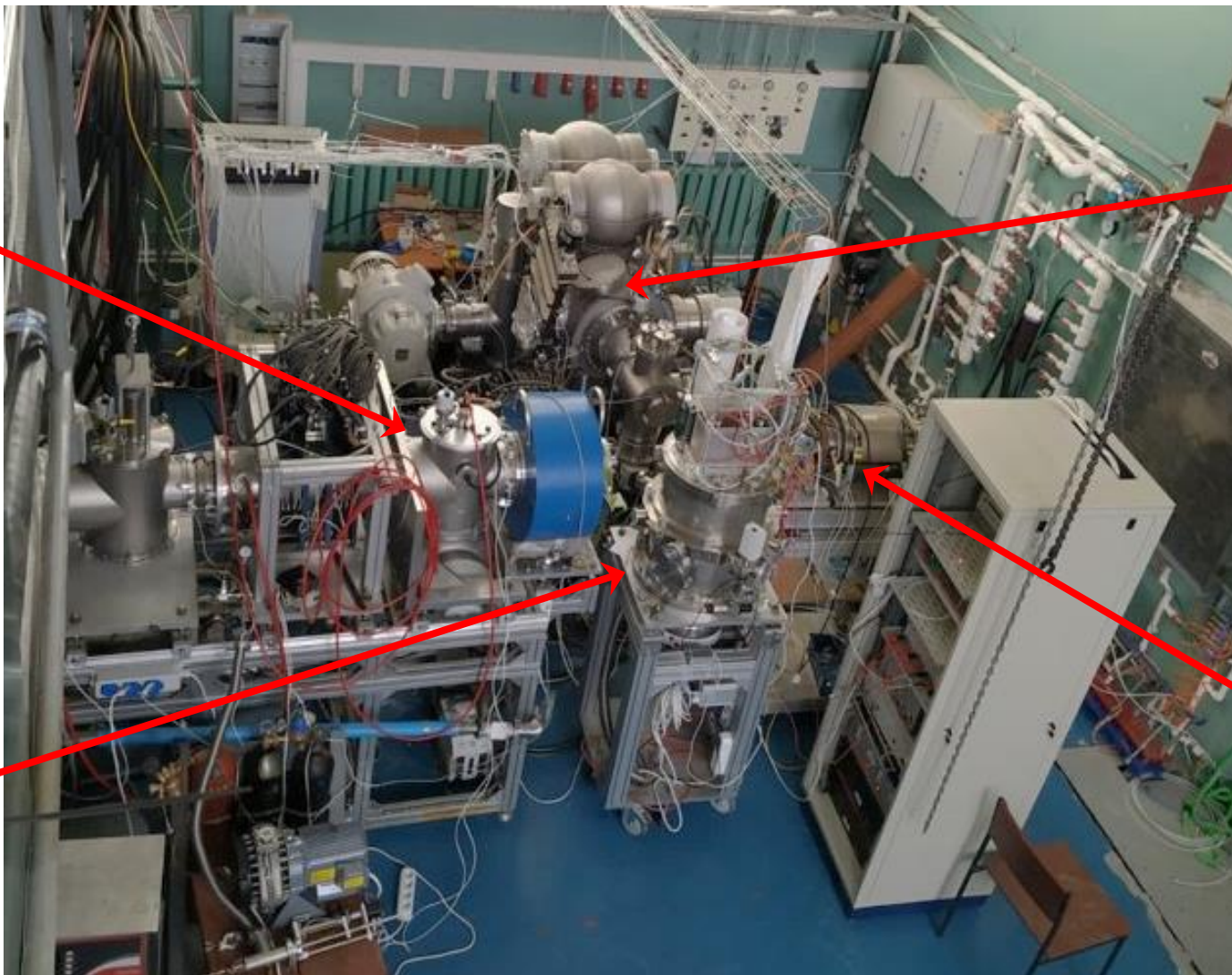
POLIS

Polarized Ion Source

Ion beam
10-50 keV
 $1.2 \cdot 10^{16}$ ions/s

Nozzle:
 $d = 1.3$ mm
 $T = 65$ K

4π – detector



PABS

Polarized Atomic Beam Source

Atomic beam
0.01 eV
 $4 \cdot 10^{16}$ atoms/s

Nozzle:
 $d = 2$ mm
 $T = 65-85$ K

NRP

Nuclear-Reaction Polarimeter

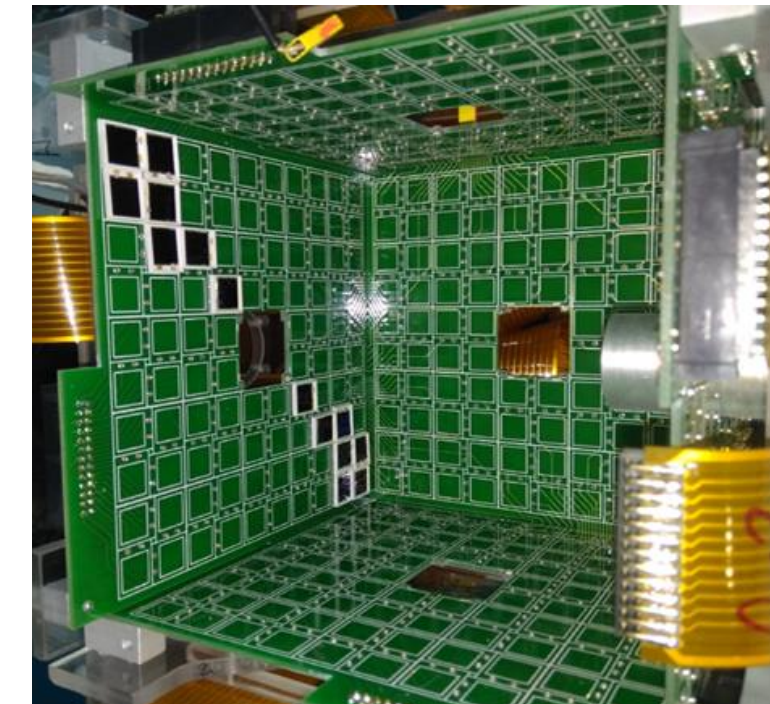
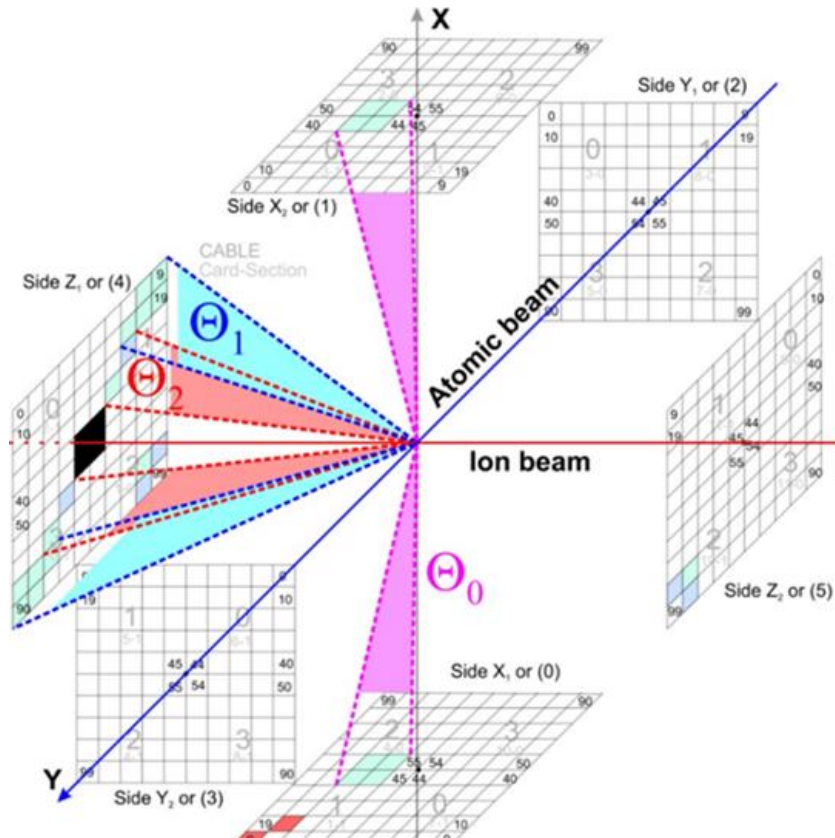


Detector system

Detector coordinate system



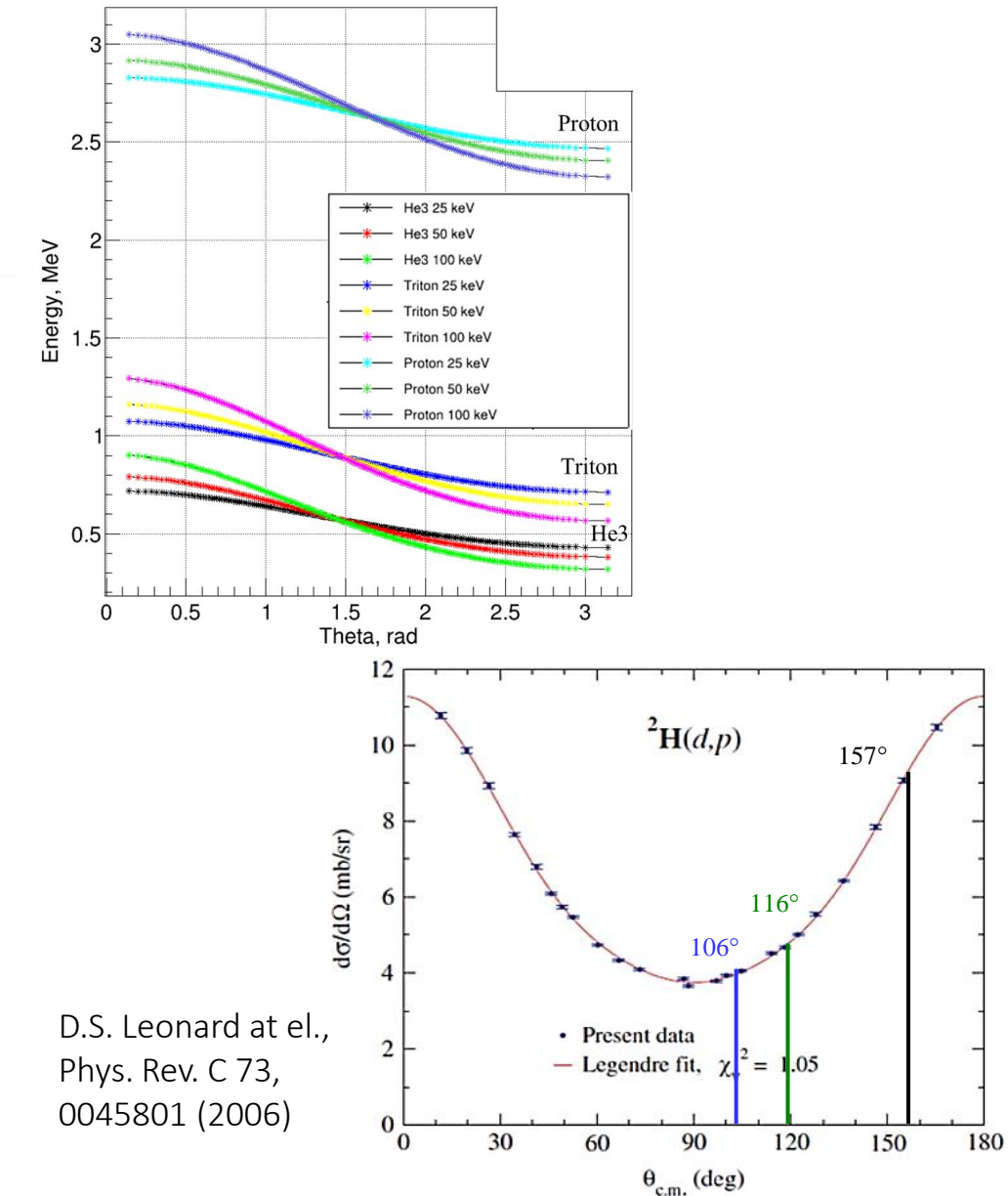
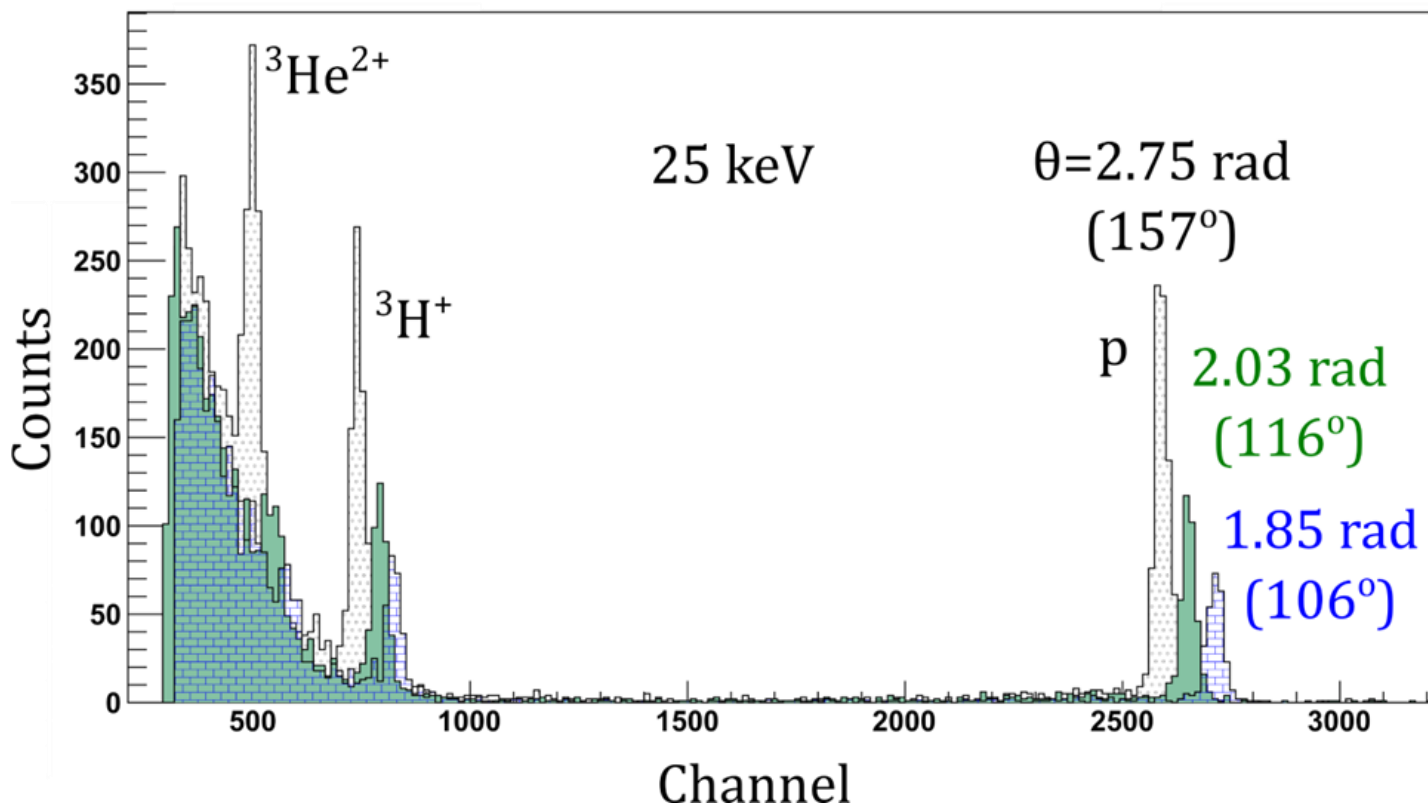
Outside view



Inside view

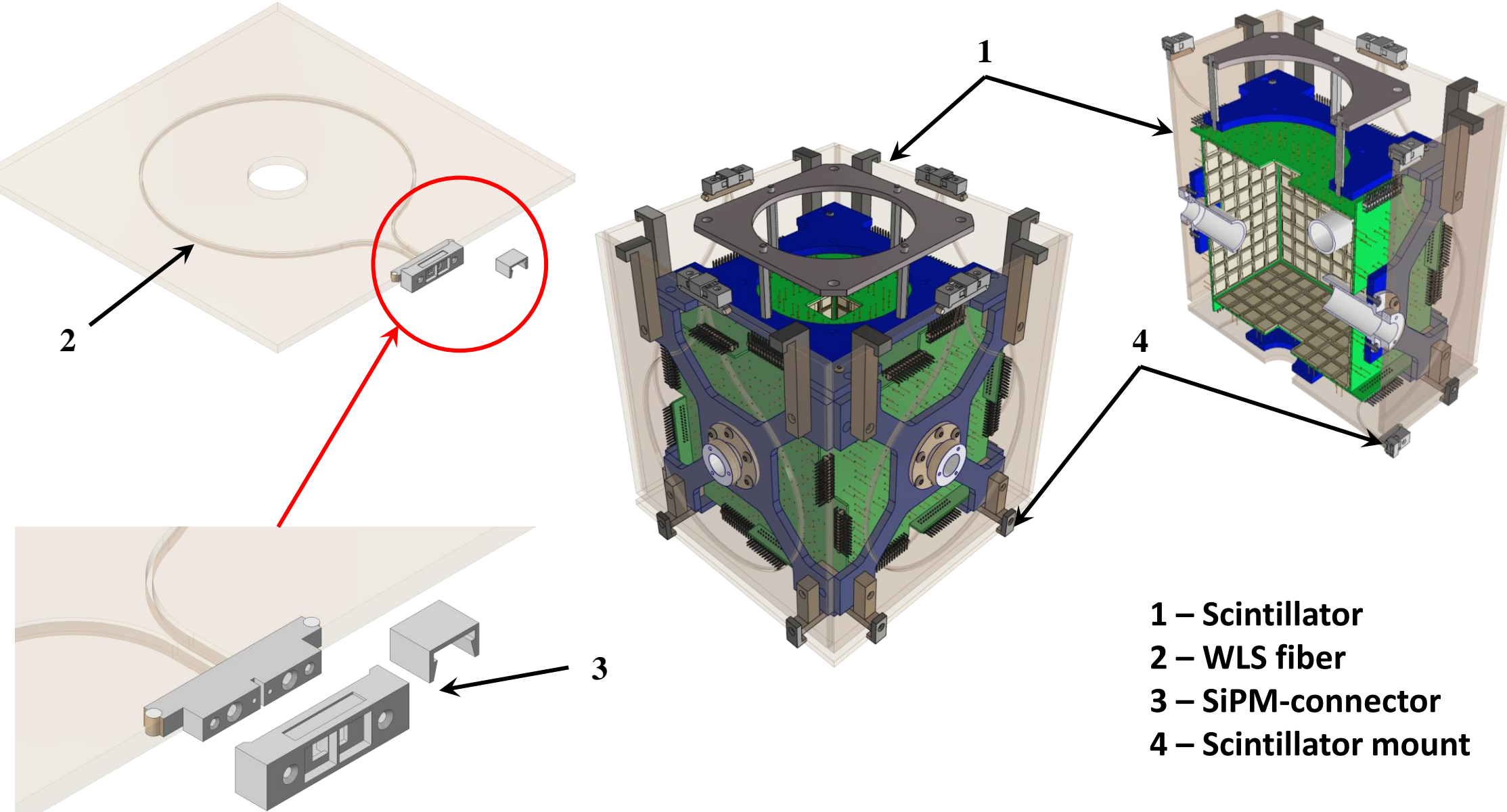


Test run 2020



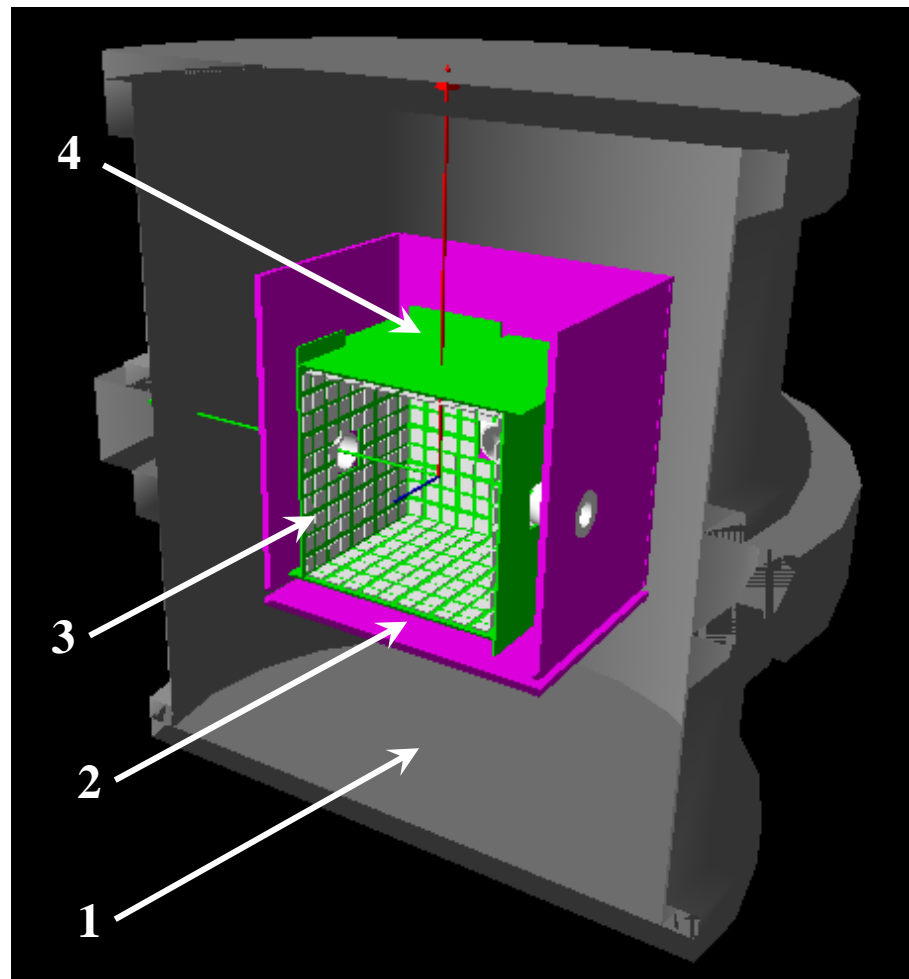


Scintillation detector

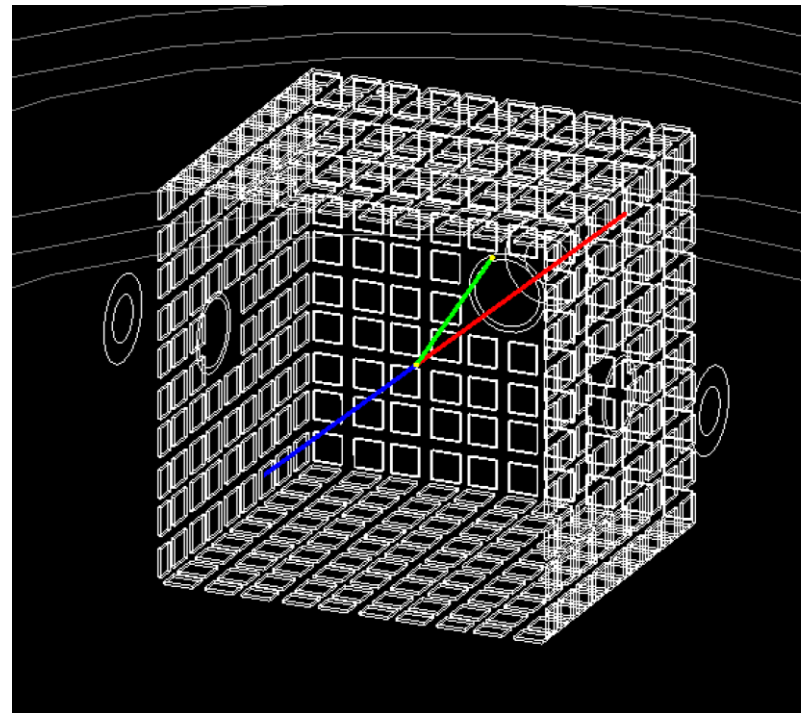




Monte-Carlo simulation in Geant 4

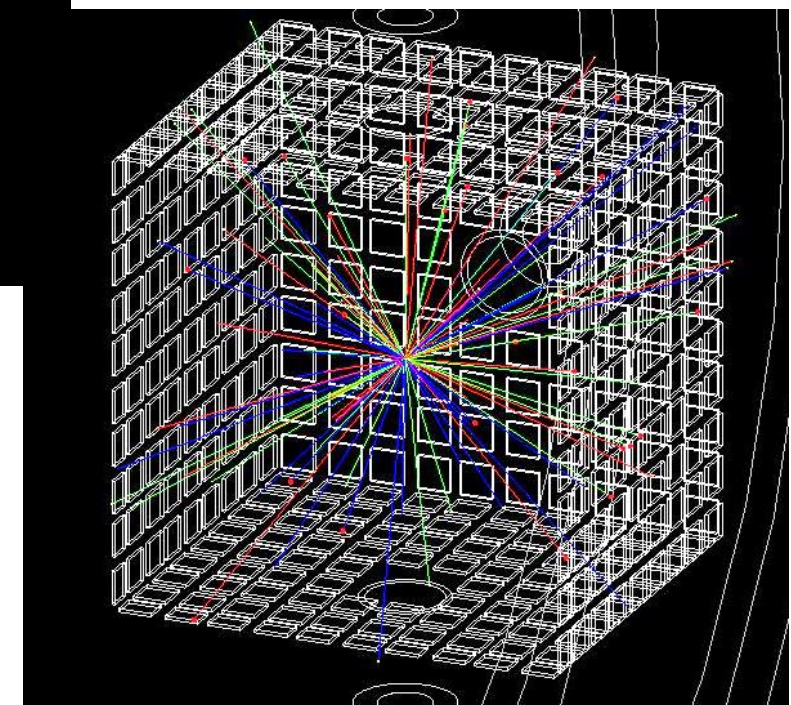


Detector geometry



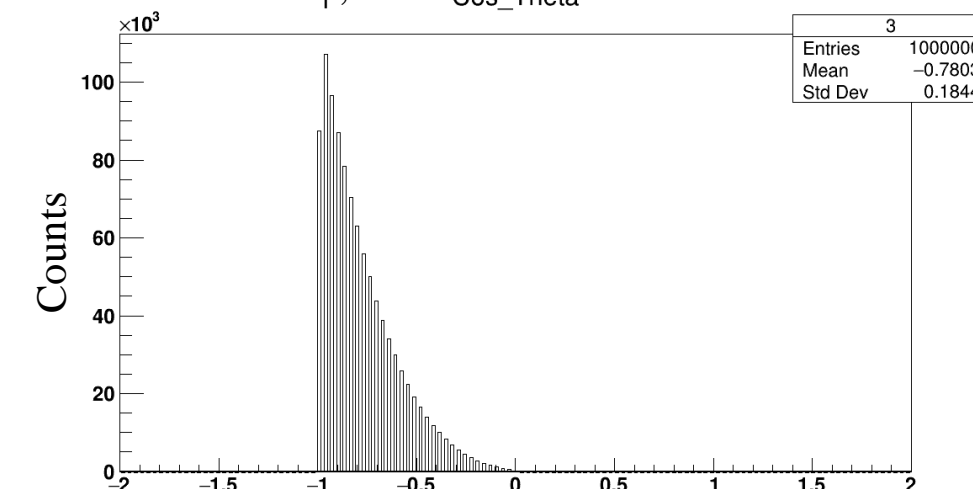
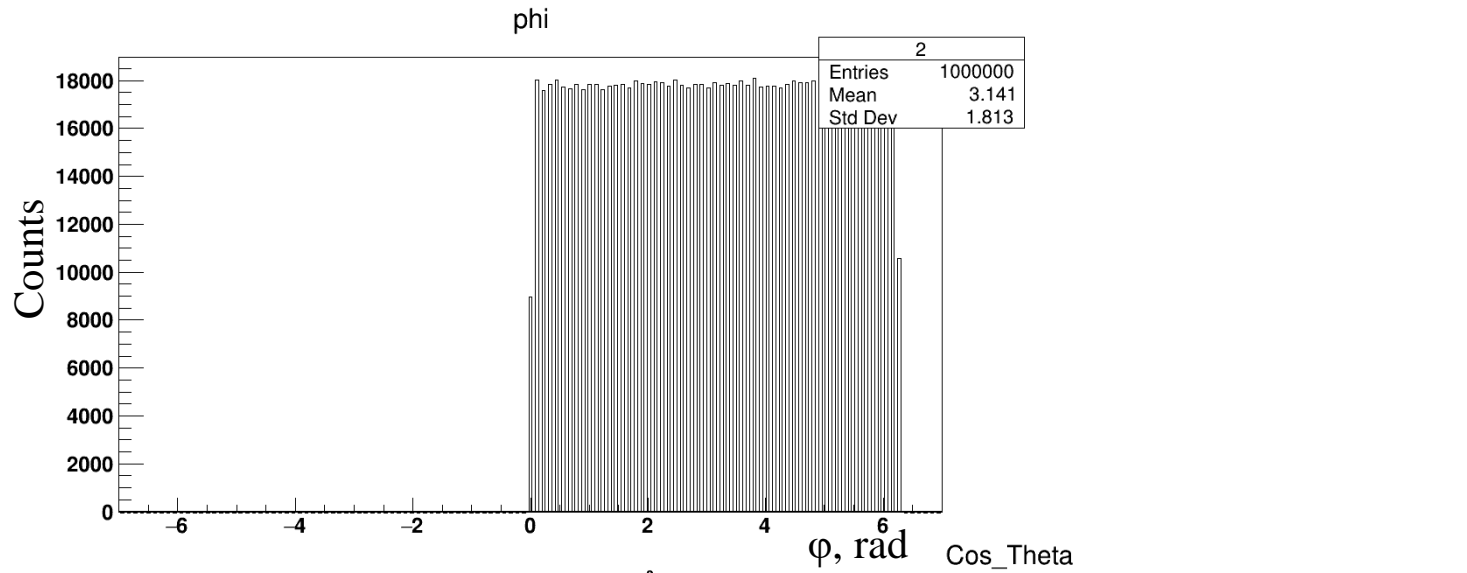
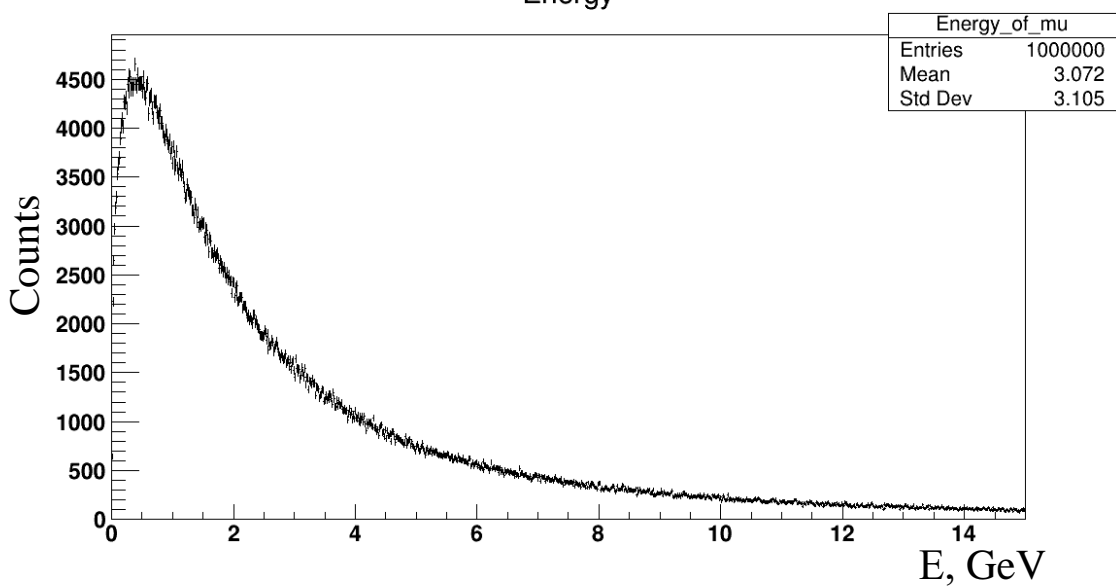
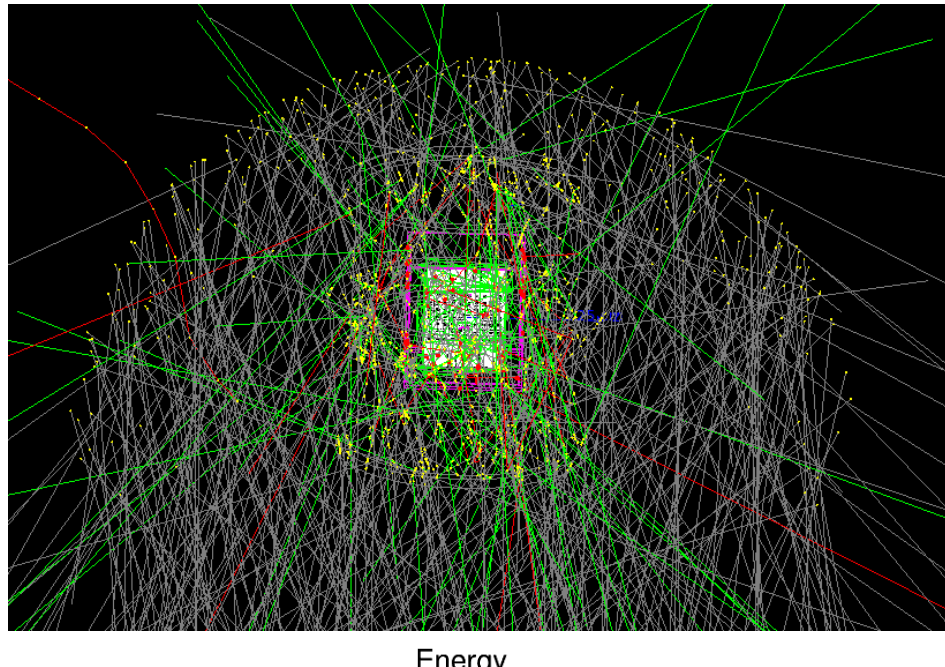
- 1 – Vacuum chamber**
- 2 – Scintillators**
- 3 – PIN - diodes**
- 4 – Printed circuit boards**

Red - p
Blue – t
Green – He3





Cosmic muon generator

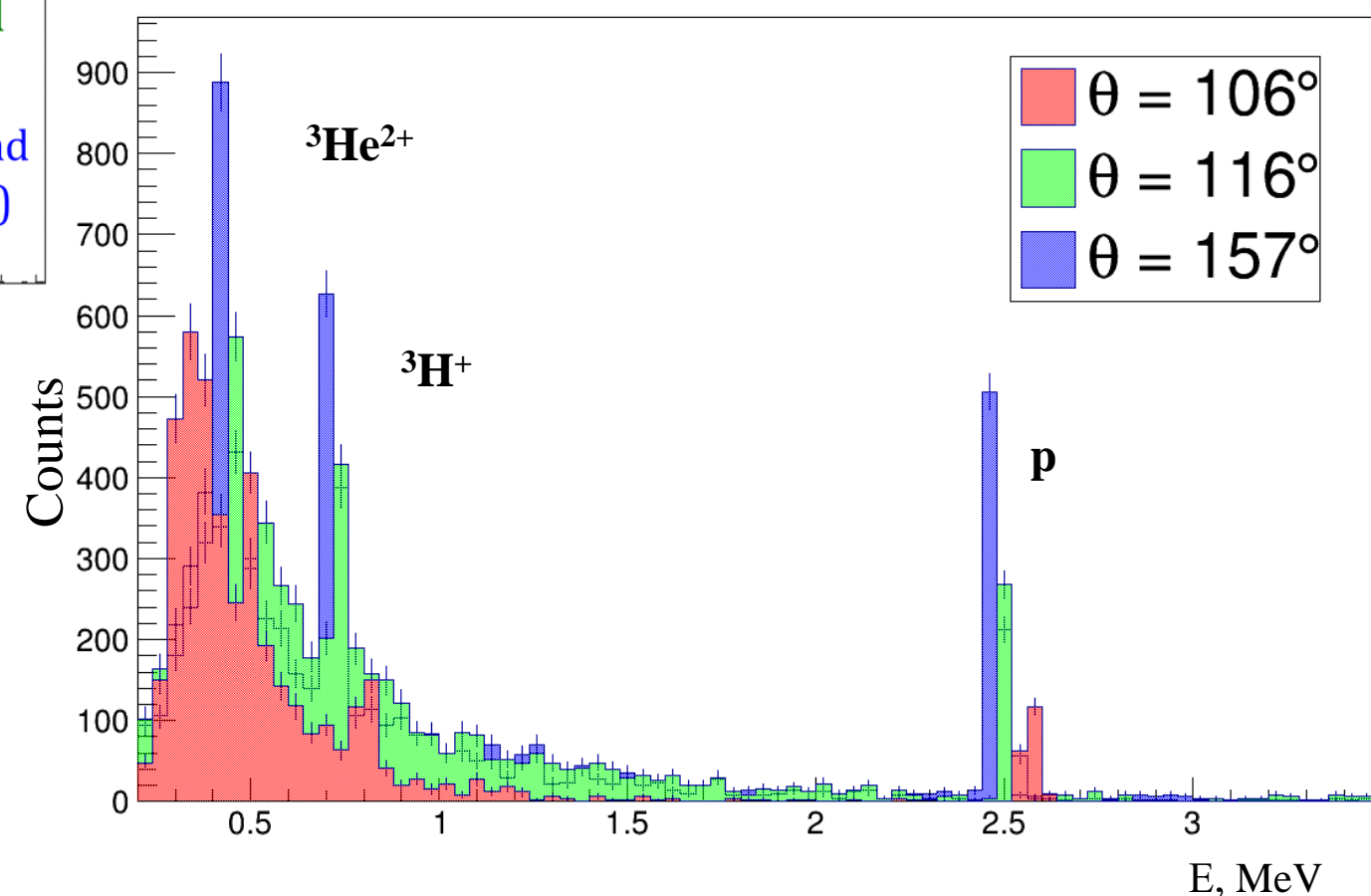
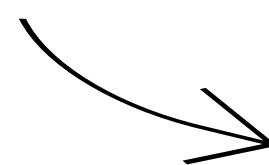
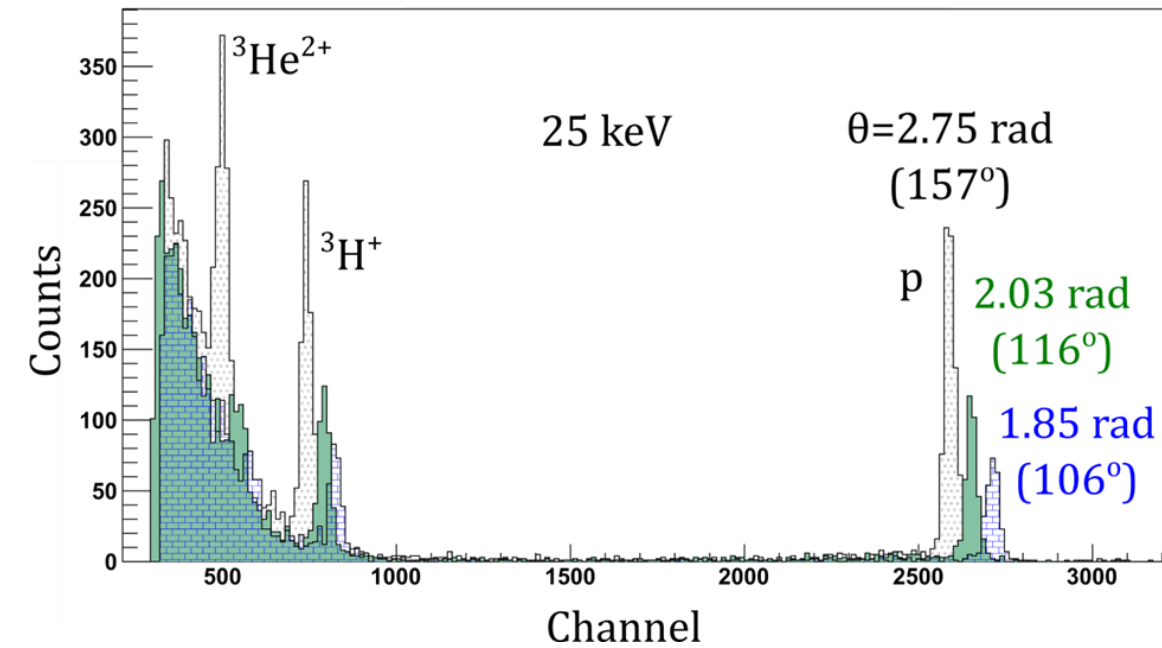


D. Pagano, et al.,
EcoMug: An Efficient COsmic MUon Generator for cosmic-ray muon applications, Nuclear
Instruments and Methods in Physics Research Section A: Accelerators, Spectrometers, Detectors
and Associated Equipment, Volume 1014, 2021, 165732, ISSN 0168-9002,
<https://doi.org/10.1016/j.nima.2021.165732>.

Anton Rozhdestvenskij



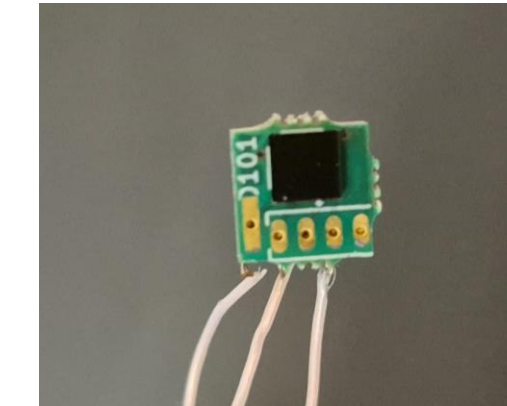
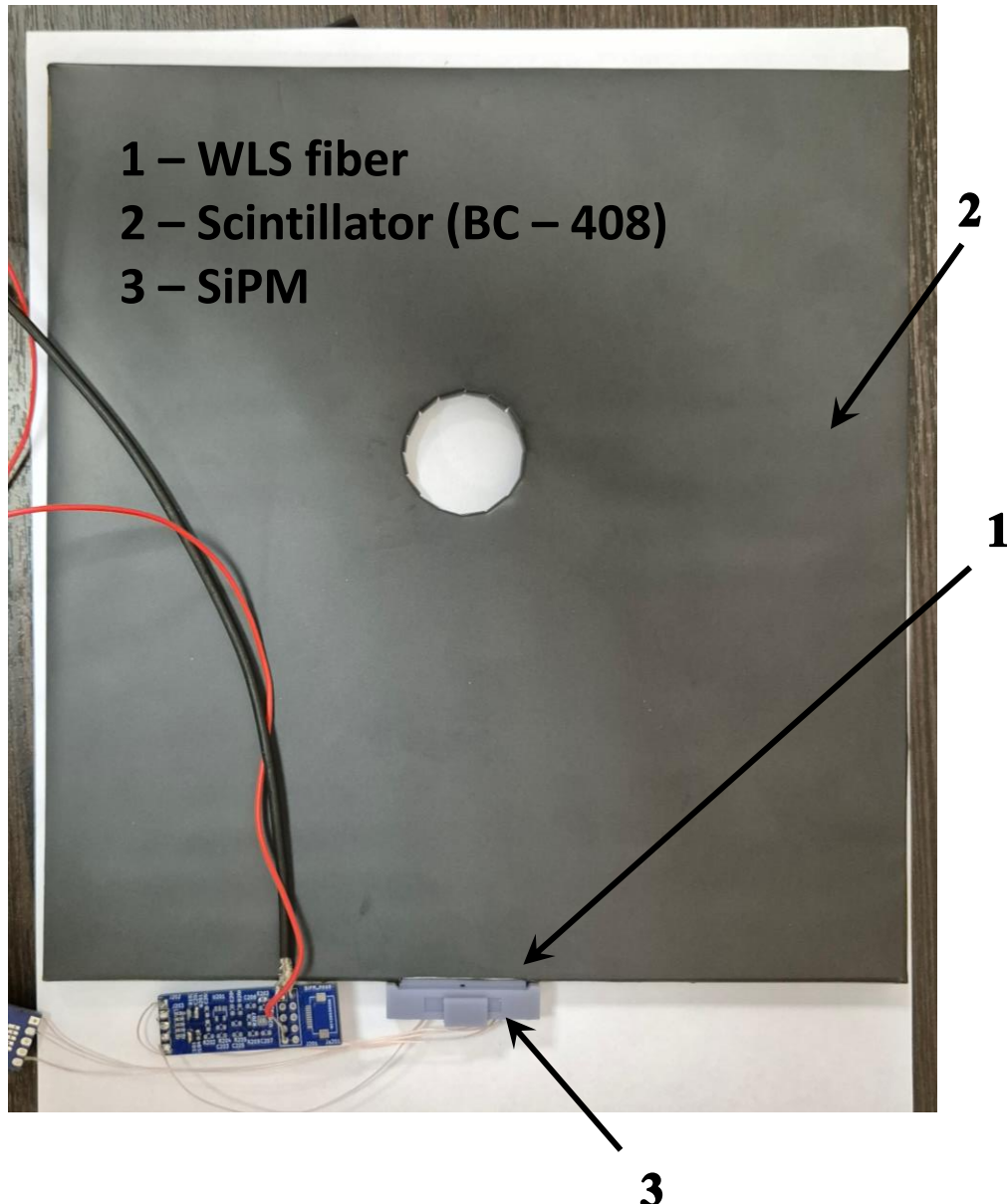
Simulation results



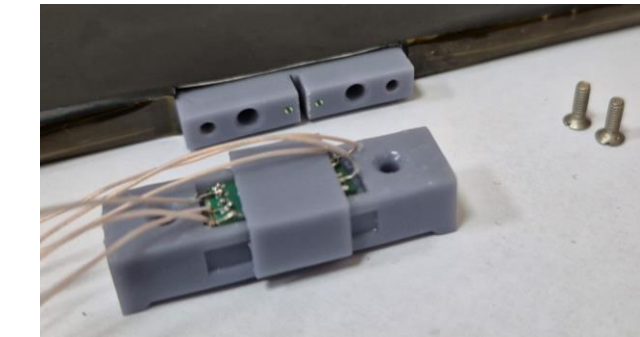
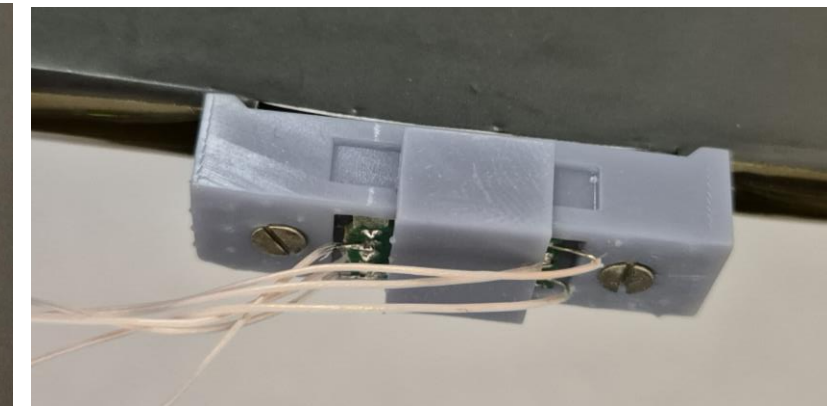


Test system

- 1 – WLS fiber
2 – Scintillator (BC – 408)
3 – SiPM

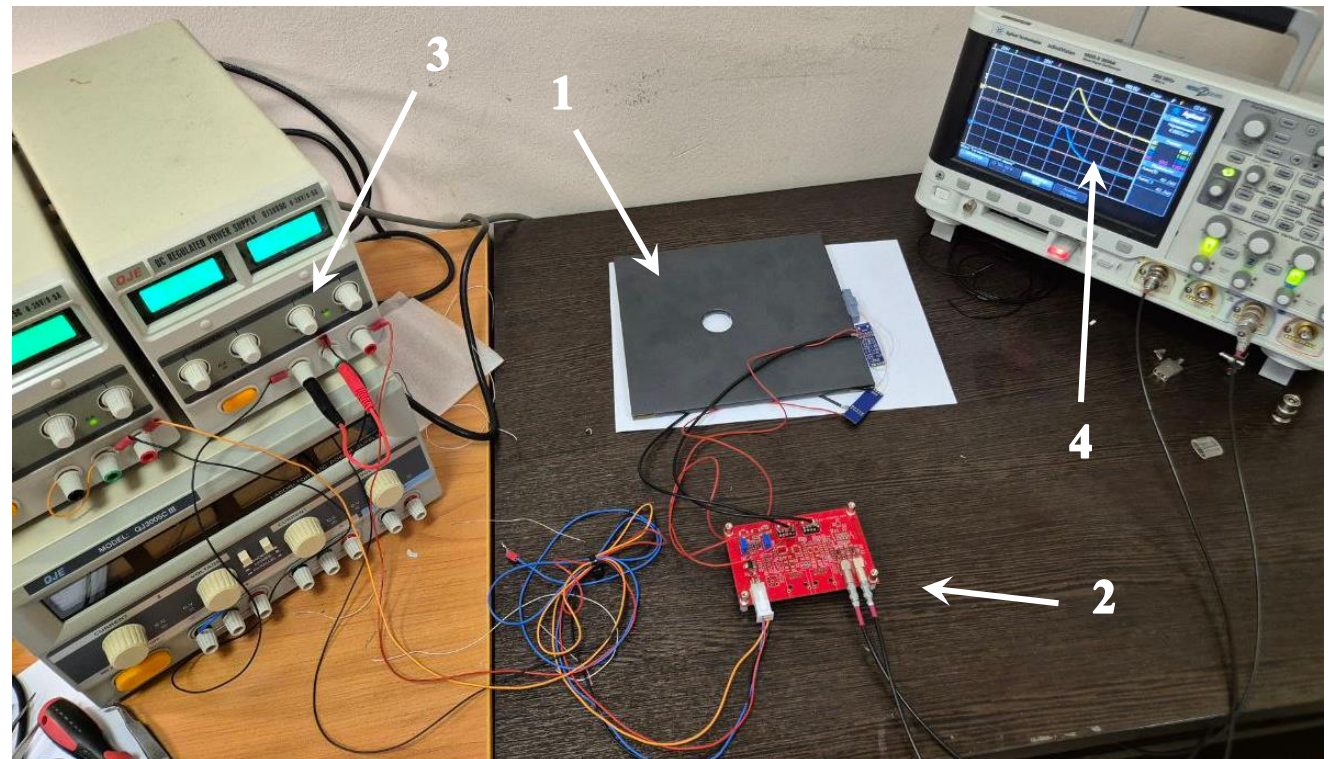


SiPM Onsemi MicroFJ-30035-TSV



WLS fiber holders and SiPM mounts

Cosmic muons registration



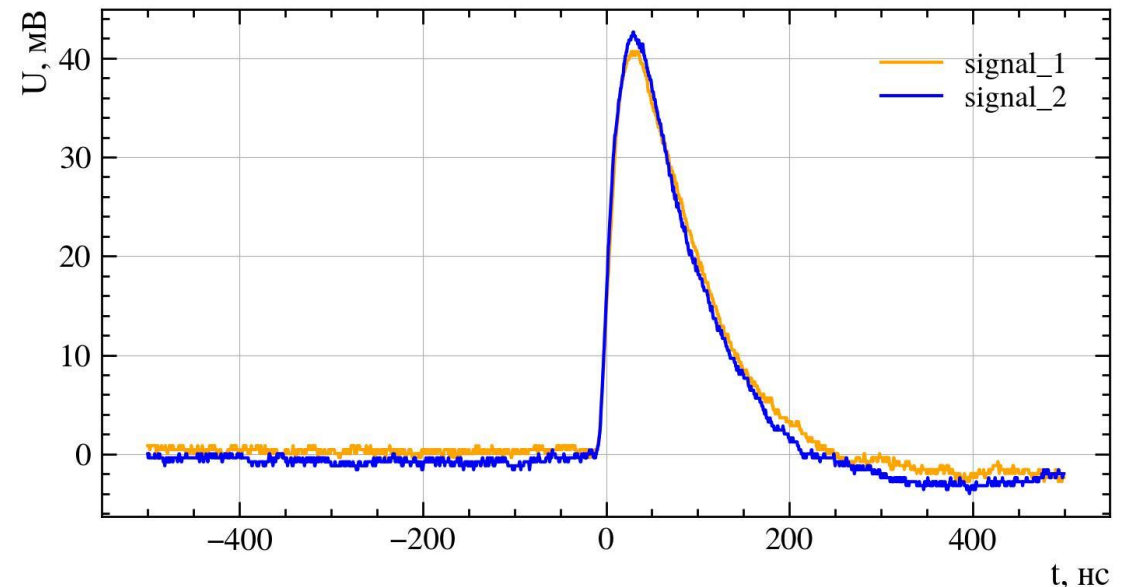
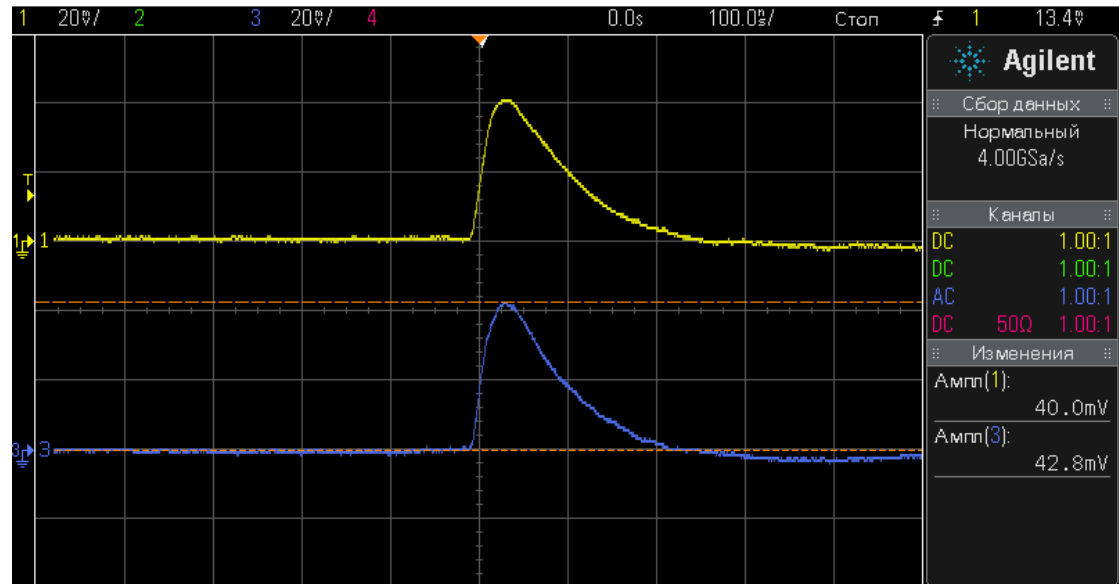
Test assembly for registration of cosmic radiation

1 – Scintillator

2 – Amplifier and power supply PCB

3 – DC voltage sources

4 – Oscilloscope

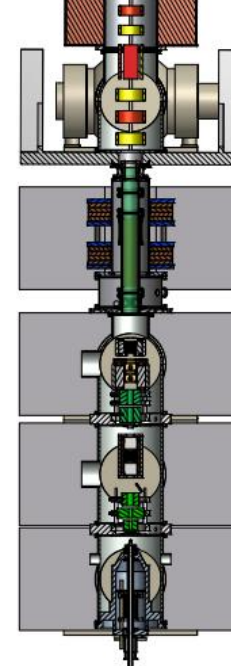
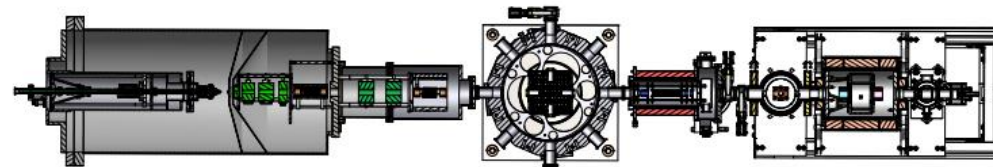




Development strategy

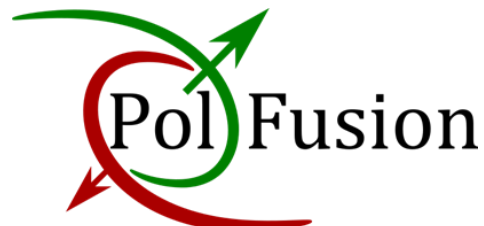
Performed:

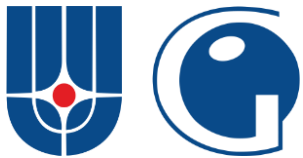
- ✓ Modelling of the scintillation detector system was carried out
- ✓ Optimal cosmic ray generator was selected
- ✓ Designed electronics for SiPM
- ✓ A test system was assembled



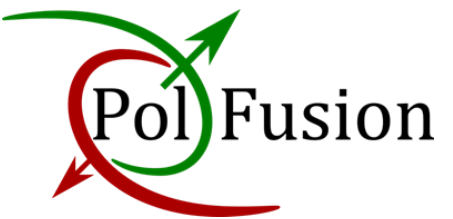
Work Plan:

- Assembly of the system outside the vacuum chamber
- Connecting the system to a common data acquisition system
- Recruitment of cosmic ray statistics
- Placing the system in the vacuum chamber of the main detector
- Obtaining experimental data



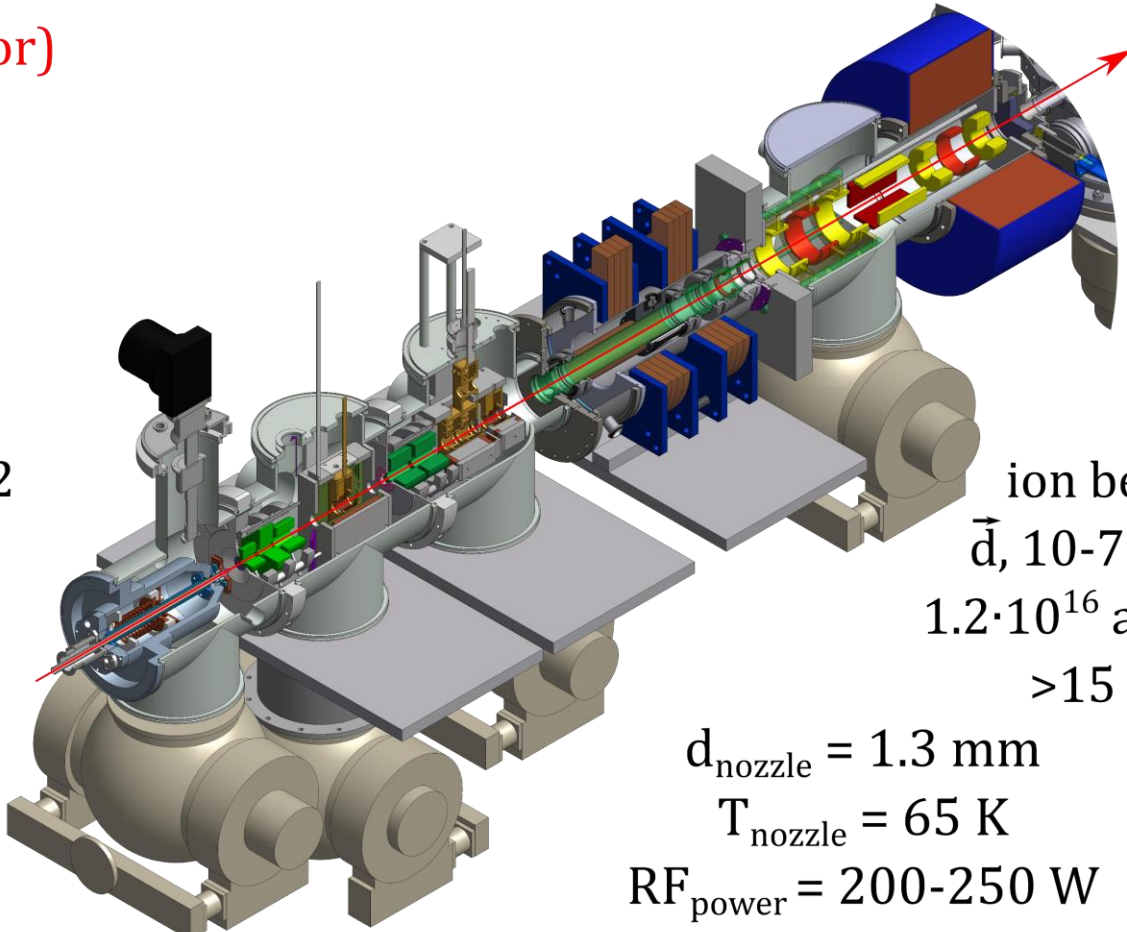
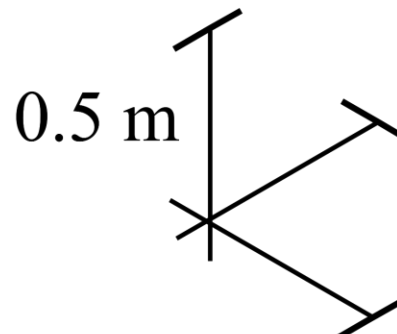


PNPI - NRC KI



Thank you for your attention!

p_z (vector)	p_{zz} (tensor)
$\pm 2/3$	0
0	+1
0	-2
$-1/3$	± 1
$+1/3$	± 1
$\pm 1/3$	$-1/2$



ion beam
 $\vec{d}, 10\text{-}75 \text{ keV}$
 $1.2 \cdot 10^{16} \text{ atoms/s}$
 $>15 \mu\text{A}$

$d_{\text{nozzle}} = 1.3 \text{ mm}$

$T_{\text{nozzle}} = 65 \text{ K}$

$\text{RF}_{\text{power}} = 200\text{-}250 \text{ W}$

Polarizer:

Sextupoles + WFT + Sextupoles + WFT + SFT1 (460 MHz) +SFT2 (350 MHz)

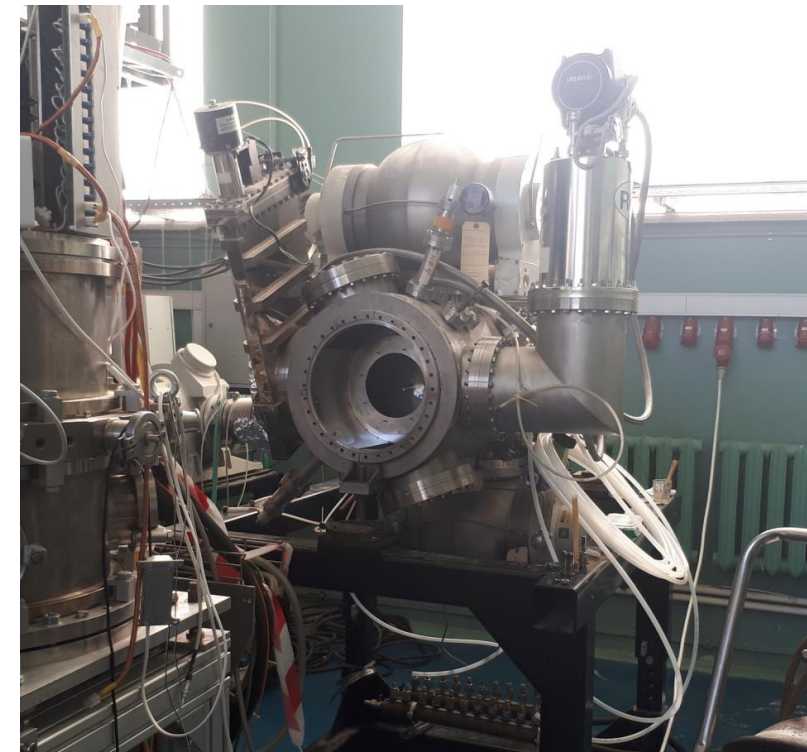
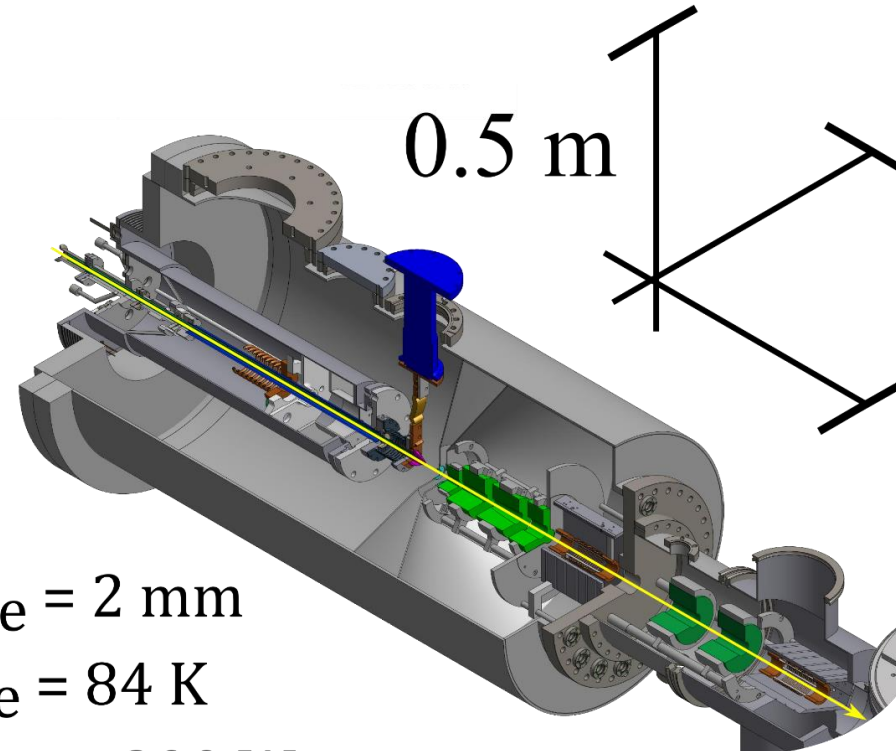


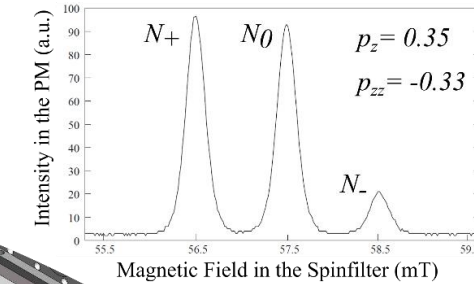
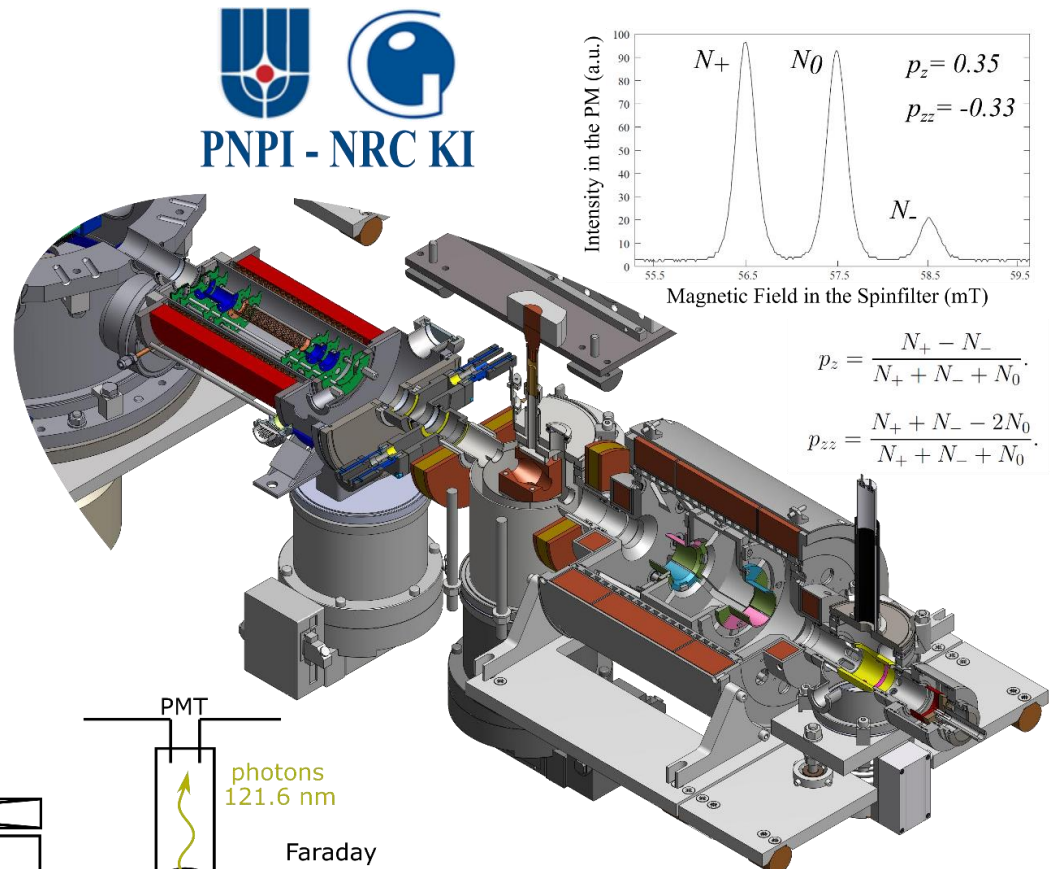
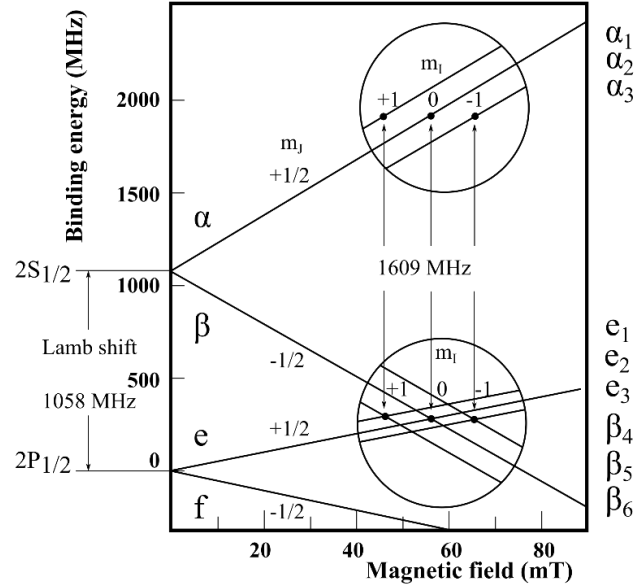
p_z (vector)	p_{zz} (tensor)
-2/3	0
0	+1
-1/3	+1
-1	+1
$\pm 1/2$	-1/2

atomic beam $d_{\text{nozzle}} = 2 \text{ mm}$
 $\vec{D}, 0.01 \text{ eV}$ $T_{\text{nozzle}} = 84 \text{ K}$
 $2 \cdot 10^{16} \text{ atoms/s}$ RF power = 300 W

Polarizing system:

Sextupoles + Quadrupoles + MFT + Sextupoles + MFT





$$p_z = \frac{N_+ - N_-}{N_+ + N_- + N_0}.$$

$$p_{zz} = \frac{N_+ + N_- - 2N_0}{N_+ + N_- + N_0}.$$

$$\frac{L - R}{L + R} = \frac{\frac{3}{2}P_Z \sin \beta A_y}{1 + \frac{1}{2}P_{ZZ}[\sin^2 \beta A_{yy} + \cos^2 \beta A_{zz}]}$$

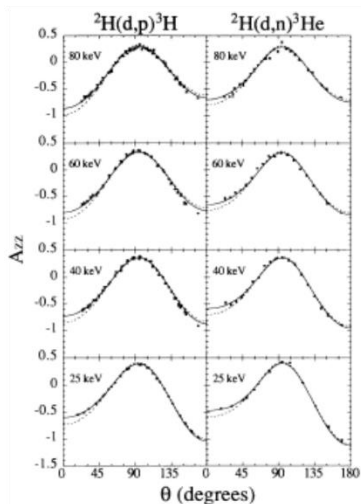
$$\frac{U - D}{U + D} = \frac{P_{ZZ} \sin \beta \cos \beta A_{xz}}{1 + \frac{1}{2}P_{ZZ}[\sin^2 \beta A_{xx} + \cos^2 \beta A_{zz}]}$$

$$\frac{2(L - R)}{L + R + U + D} = \frac{\frac{3}{2}P_Z \sin \beta A_y}{1 + \frac{1}{4}P_{ZZ}[3(\cos^2 \beta - 1)A_{zz}]}$$

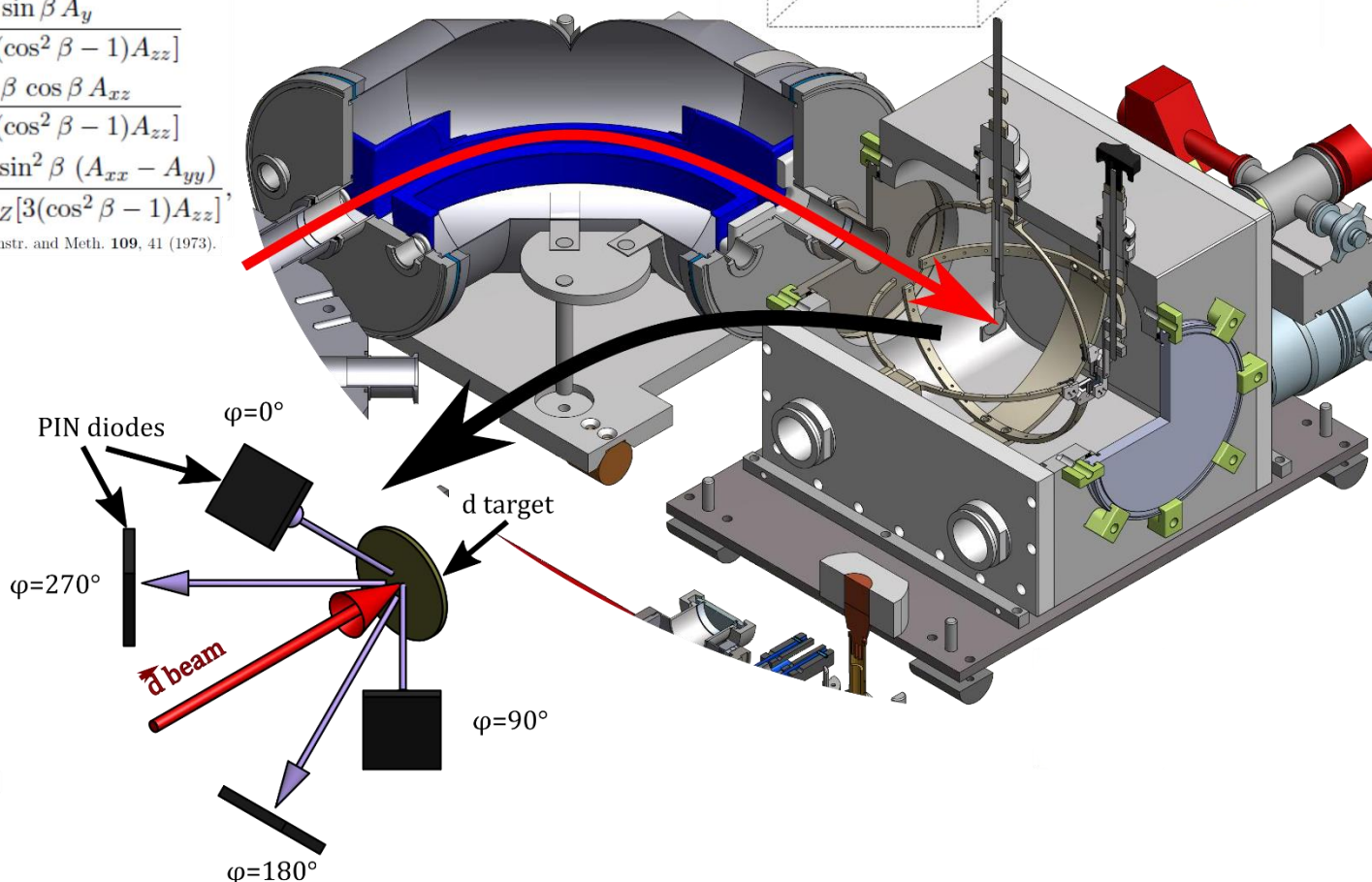
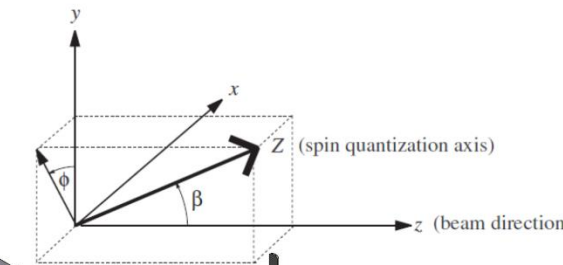
$$\frac{2(U - D)}{L + R + U + D} = \frac{P_{ZZ} \sin \beta \cos \beta A_{xz}}{1 + \frac{1}{4}P_{ZZ}[3(\cos^2 \beta - 1)A_{zz}]}$$

$$\frac{(L + R) - (U + D)}{L + R + U + D} = \frac{-\frac{1}{4}P_{ZZ} \sin^2 \beta (A_{xx} - A_{yy})}{1 + \frac{1}{4}P_{ZZ}[3(\cos^2 \beta - 1)A_{zz}]},$$

G.G. Ohlsen, P.W. Keaton, Jr., Nucl. Instr. and Meth. **109**, 41 (1973).

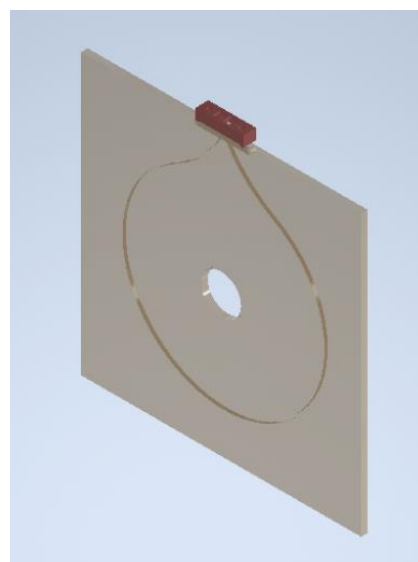
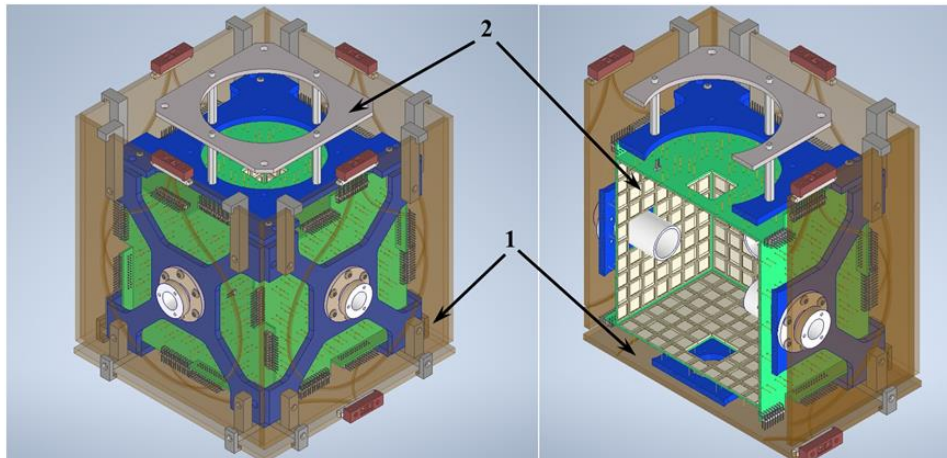
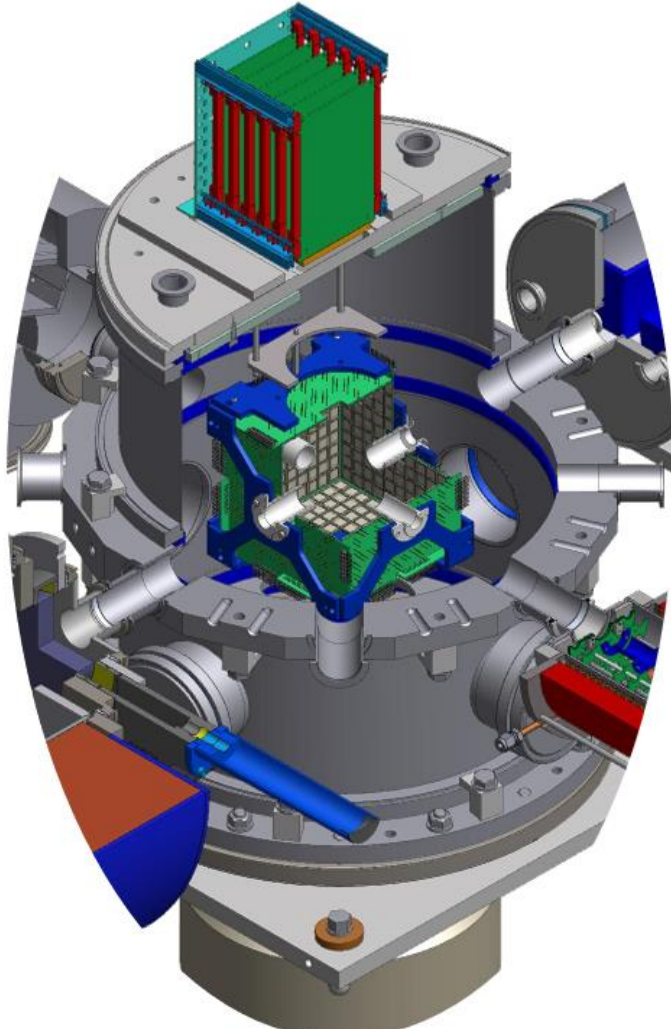


K. Fletcher, et al., Phys. Rev. C **49**, 2305 (1994).



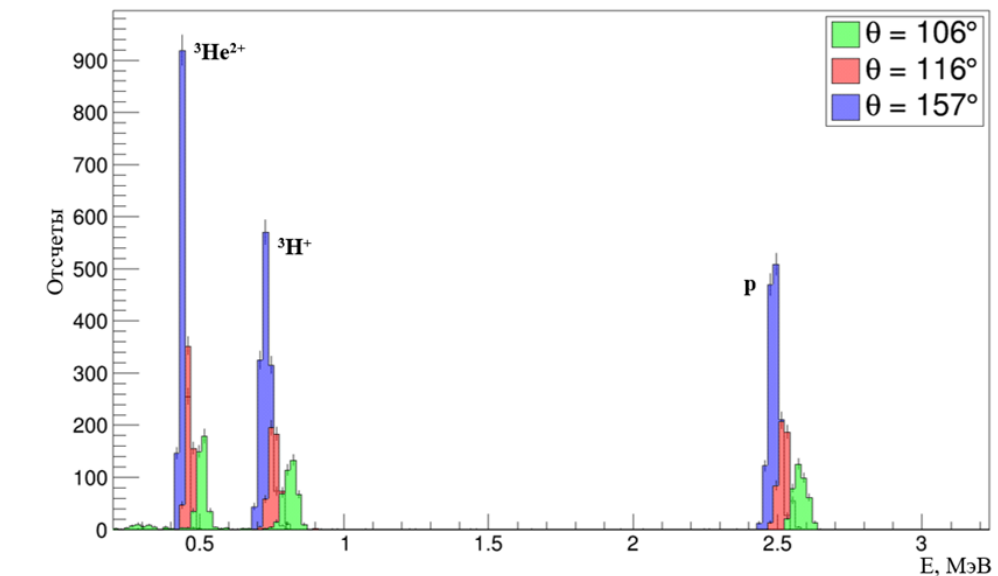
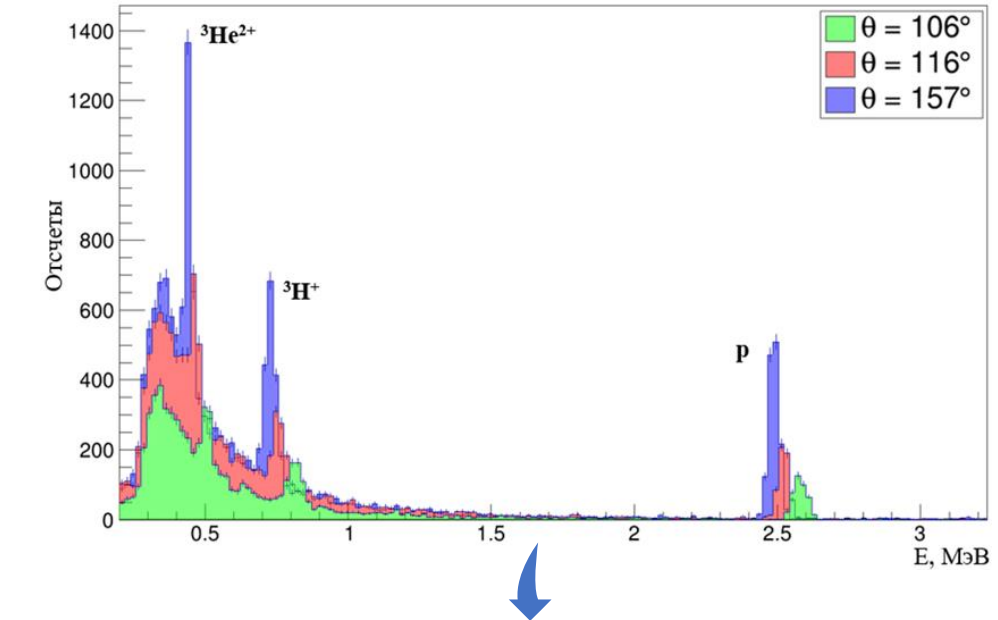
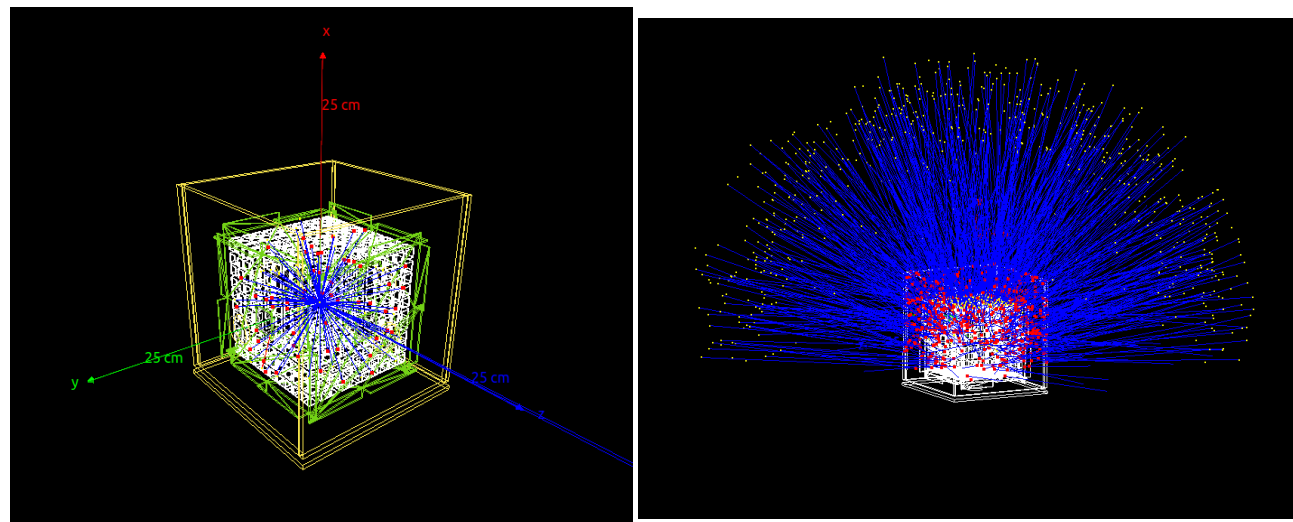
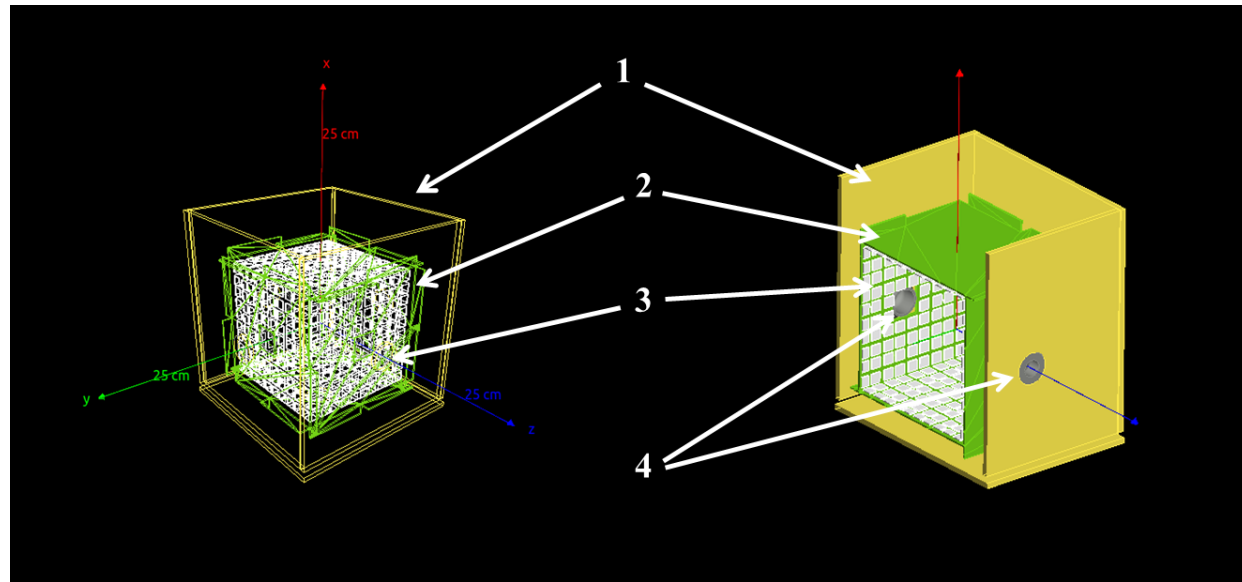


Detector system



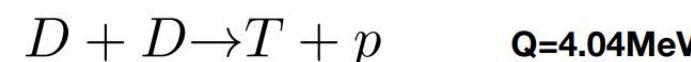
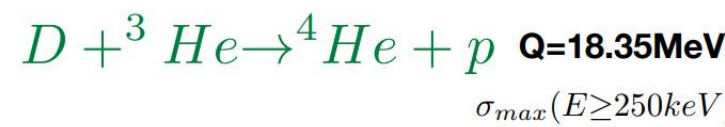
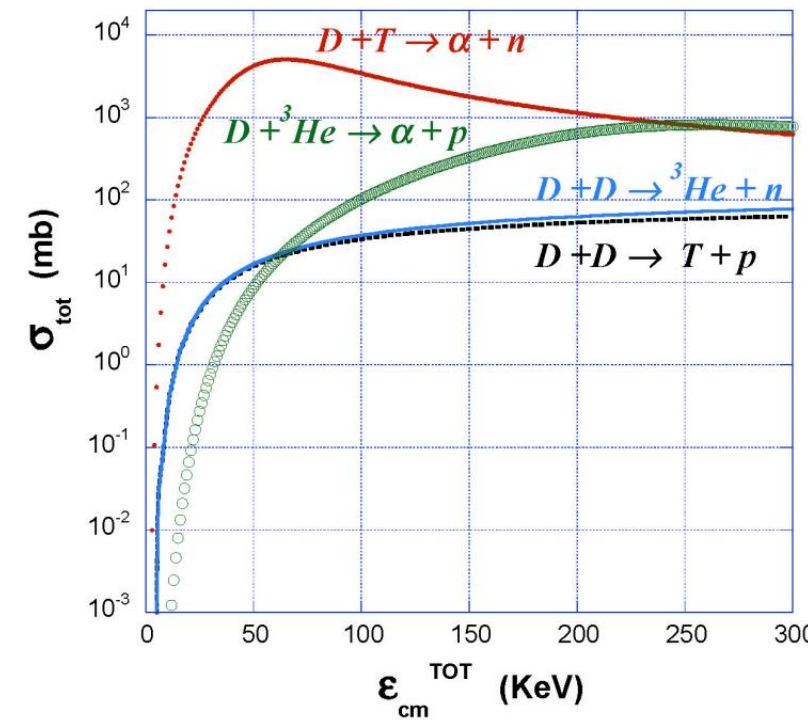
① concentrator
② top flange

③ signal cables
④ detector cube

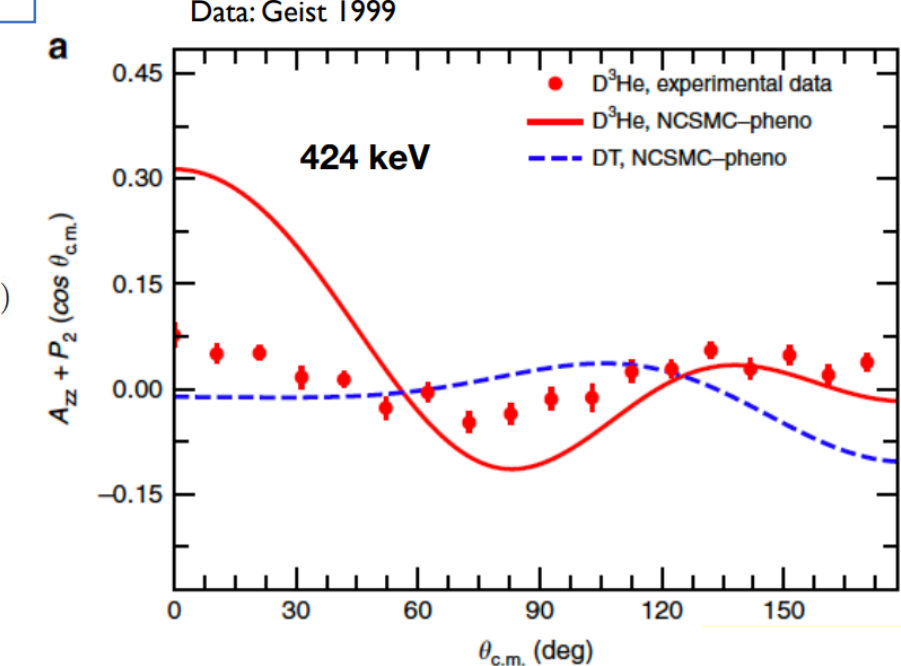




Optical polarization ${}^3\text{He}$



$\sigma_{\text{max}}(E \sim 1000\text{keV})$



G.Hupin, S.Quaglioni, P.Navratil (2019)
<https://doi.org/10.1038/s41467-018-08052-6>



Cross section

$$\begin{aligned}
\sigma(\Theta, \Phi) = \sigma_0(\Theta) \{ & 1 + \frac{3}{2} [A_y^{(b)}(\Theta)p_y + A_y^{(t)}q_y] + \frac{1}{2} [A_{zz}^{(b)}(\Theta)p_{zz} + A_{zz}^{(t)}(\Theta)q_{zz}] \\
& + \frac{1}{6} [A_{xx-yy}^{(b)}(\Theta)p_{xx-yy} + A_{xx-yy}^{(t)}(\Theta)q_{xx-yy}] \\
& + \frac{2}{3} [A_{xz}^{(b)}(\Theta)p_{xz} + A_{xz}^{(t)}(\Theta)q_{xz}] \\
& + \frac{9}{4} [C_{y,y}(\Theta)p_yq_y + C_{x,x}(\Theta)p_xq_x + C_{x,z}(\Theta)p_xq_z \\
& \quad + C_{z,x}(\Theta)p_zq_x + C_{z,z}(\Theta)p_zq_z] \\
& + \frac{3}{4} [C_{y,zz}(\Theta)p_yq_{zz} + C_{zz,y}(\Theta)p_{zz}q_y] \\
& + C_{y,zz}(\Theta)p_yq_{xz} + C_{xz,y}(\Theta)p_{xz}q_y + C_{x,yz}(\Theta)p_xq_{yz} \\
& + C_{yz,x}(\Theta)p_{yz}q_x + C_{z,yz}(\Theta)p_zq_{yz} + C_{yz,z}(\Theta)p_{yz}q_z \\
& + \frac{1}{4} [C_{y,xx-yy}(\Theta)p_yq_{xx-yy} + C_{xx-yy,y}(\Theta)p_{xx-yy}q_y \\
& \quad + C_{zz,zz}(\Theta)p_{zz}q_{zz}] \\
& + \frac{1}{3} [C_{zz,xz}(\Theta)p_{zz}q_{xz} + C_{xz,zz}(\Theta)p_{xz}q_{zz}] \\
& + \frac{1}{12} [C_{zz,xx-yy}(\Theta)p_{zz}q_{xx-yy} + C_{xx-yy,zz}(\Theta)p_{xx-yy}q_{zz}] \\
& + \frac{4}{9} [C_{xz,xz}(\Theta)p_{xz}q_{xz} + C_{yz,yz}(\Theta)p_{yz}q_{yz}] \\
& + \frac{8}{9} [C_{xy,yz}(\Theta)p_{xy}q_{yz} + C_{yz,xy}(\Theta)p_{yz}q_{xy}] \\
& + \frac{16}{9} C_{xy,xy}(\Theta)p_{xy}q_{xy} \\
& + \frac{1}{9} [C_{xz,xx-yy}(\Theta)p_{xz}q_{xx-yy} + C_{xx-yy,xz}(\Theta)p_{xx-yy}q_{xz}] \\
& + \frac{1}{36} C_{xx-yy,xx-yy}(\Theta)p_{xx-yy}q_{xx-yy} \\
& + \frac{1}{2} [C_{x,xy}(\Theta)p_xq_{xy} + C_{xy,x}(\Theta)p_{xy}q_x + C_{z,xy}(\Theta)p_zq_{xy} \\
& \quad + C_{xy,z}(\Theta)p_{xy}q_z] \}
\end{aligned}$$

The spins of both deuterons are the same:
Only $p_z(q_z)$ and $p_{zz}(q_{zz}) \neq 0$

$$\begin{aligned}
\sigma(\Theta, \Phi) = \sigma_0(\Theta) \{ & 1 + \frac{3}{2} [A_{zz}^{(b)}(\Theta)p_{zz} + A_{zz}^{(t)}(\Theta)q_{zz}] \\
& + \frac{9}{4} C_{z,z}(\Theta)p_zq_z + \frac{1}{4} C_{zz,zz}(\Theta)p_{zz}q_{zz} \}
\end{aligned}$$

Polarized beam ($p_{i,j} \neq 0, q_{i,j} = 0$):

$$\begin{aligned}
\sigma(\Theta, \Phi) = \sigma_0(\Theta) \cdot & \{ 1 + 3/2 A_y(\Theta) p_y + 1/2 A_{xz}(\Theta) p_{xz} \\
& + 1/6 A_{xx-yy}(\Theta) p_{xx-zz} \\
& + 2/3 A_{zz}(\Theta) p_{zz} \}
\end{aligned}$$